

DOKUZ EYLÜL UNIVERSITY
GRADUATE SCHOOL OF NATURAL AND APPLIED SCIENCES

**WIDE-BAND ANTENNA DESIGN AND
IMPLEMENTATION
FOR
SMALL-SIZE RF ANECHOIC CHAMBERS**

by
Mehmet Can ÖZGÖNÜL

December, 2015

İZMİR

**WIDE-BAND ANTENNA DESIGN AND
IMPLEMENTATION
FOR
SMALL-SIZE RF ANECHOIC CHAMBERS**

**A Thesis Submitted to the
Graduate School of Natural and Applied Sciences of Dokuz Eylül University
In Partial Fulfillment of the Requirements for the Degree of Master of Sciences
in Electrical and Electronics Engineering Program**

**by
Mehmet Can ÖZGÖNÜL**

December, 2015

İZMİR

M.Sc THESIS EXAMINATION RESULT FORM

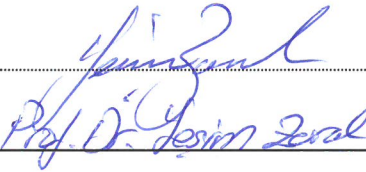
We have read the thesis entitled “**WIDE-BAND ANTENNA DESIGN AND IMPLEMENTATION FOR SMALL-SIZE RF ANECHOIC CHAMBERS**” completed by **MEHMET CAN ÖZGÖNÜL** under supervision of **ASSIT.PROF.DR. AHMET ÖZKURT** and **ASSOC.PROF.DR. MUSTAFA SEÇMEN** and we certify that in our opinion it is fully adequate, in scope and in quality, as thesis for the degree of Master of Science.


Assist. Prof. Dr. Ahmet ÖZKURT

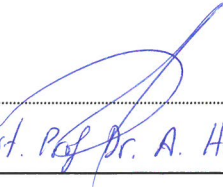
Supervisor


Assoc. Prof. Dr. Mustafa SEÇMEN

Supervisor


Prof. Dr. Yasin Zoral

Jury Member


Assist. Prof. Dr. A. Haluk Nalbantoğlu

Jury Member


Prof. Dr. Ayşe OKUR

Director

Graduate School of Natural and Applied Sciences

ACKNOWLEDGEMENT

Firstly, I would like to thank and express my sincere gratitude to Assist. Prof. Dr. Ahmet ÖZKURT and Assoc. Prof. Dr. Mustafa SEÇMEN for their guidance, kindness and encouragement during this study.

I would like to thank Prof. Dr. Yeşim ZORAL and Prof. Dr. Adnan KAYA for sharing their experiences in microwave systems.

I wish like to thank to the member of my thesis committee Assist. Prof. Dr. Ali Haluk NALBANTOĞLU for his contribution.

I also wish like to thank for my family for their endless support and unconditional love.

Lastly, I would like to thank Research Assistants, Şebnem SEÇKİN UĞURLU and Cem BAYTÖRE for their great support.

Mehmet Can ÖZGÖNÜL

WIDE-BAND ANTENNA DESIGN AND IMPLEMENTATION FOR SMALL-SIZE RF ANECHOIC CHAMBERS

ABSTRACT

In this thesis work; wideband microstrip planar monopole antennas consisting of two different types and a microstrip log periodic dipole array antenna are designed and fabricated for wireless communication systems, which are frequently used nowadays. The return loss performances of the antennas within the desired operating frequency bandwidth of 750 MHz to 3000 MHz are almost kept above about 10 dB by using circular disc in the first monopole antenna, and using step cut at four corners method to the radiated surface with T-shape slot at the ground surface of the rectangular patch in the second monopole. Then, a log periodic dipole array antenna is designed to operate at wideband by the help of the standard formulations for log periodic array. In this way, these antennas become convenient for the systems of Global System for Mobile Communication (900 MHz), Global Positioning System (1227 MHz, 1575 MHz), Third Generation of Mobile Telecommunications Technology (2100 MHz), Wireless Fidelity (2400 MHz) and Long Term Evolution (2600 MHz). Besides, these antennas are designed according to the dimensions of a small-size anechoic chamber at the Antenna and Microwave Technique Laboratory of Dokuz Eylül University which is a setup in order to measure the performances of the antennas and systems within the described frequency bandwidth, and they are considered to be used in this chamber. Finally, a Koch Fractal log periodic dipole array antenna is designed, simulated and manufactured.

Keywords: Microstrip planar monopole antenna, log periodic dipole array antenna, small-size anechoic chamber, wireless communication

KÜÇÜK BOYUTLU RF YANSITMASIZ ODALAR İÇİN GENİŞ BAND ANTEN TASARIMI VE UYGULAMASI

ÖZ

Bu tez çalışmasında; günümüzde yaygın olarak kullanılan kablosuz haberleşmenin çeşitli türleri için uygun geniş bantlı, iki farklı tipte mikroşerit düzlemsel monopol antenler ve mikroşerit log periyodik dipol dizi anten tasarlanmış ve üretilmiştir. İlk monopol antende yuvarlak disk kullanılarak, ikinci monopol antende ise mikroşerit dikdörtgen yamanın ışımaya yapan yüzeyine dört köşesinden kesme yöntemi kullanılarak ve toprak yüzeyine T-şeklinde yarık ile, antenlerin istenilen çalışma frekans aralığı olan 750 MHz ile 3000 MHz aralığında geri dönüş kaybı performansları neredeyse 10 dB seviyesinin üstünde tutulmuştur. Daha sonra, bir log periyodik dipol dizi anten, log periyodik dipol dizi için olan standart formüller yardımıyla geniş bandta çalışacak şekilde tasarlanmıştır. Böylece bu antenler; Mobil İletişim için Küresel Sistem (900 MHz), Küresel Konumlama Sistemi (1227 MHz ve 1575 MHz), Üçüncü Nesil Mobil Telekomünikasyon Teknolojisi (2100 MHz), Kablosuz Bağlantı Alanı (2400 MHz), ve Uzun Süreli Gelişim (2600 MHz) sistemleri için uygun hale gelmiştir. Ayrıca bu antenler, belirtilen frekans bandı aralığındaki antenlerin ve sistemlerin performanslarını ölçmek amacıyla Dokuz Eylül Üniversitesi Anten ve Mikrodalga Tekniği Laboratuvarında kurulan küçük boyutlu yansıtmasız odanın boyutlarına göre tasarlanmıştır ve bu odada kullanması düşünülmektedir. Son olarak, Koch Fraktal log periyodik dipol dizi anten tasarlanmış, simülasyonu gerçekleştirilmiş ve üretilmiştir..

Anahtar kelimeler: Mikroşerit düzlemsel monopol anten, log periyodik dipol dizi anten, küçük boyutlu yansıtmasız oda, kablosuz haberleşme

CONTENTS

	Page
THESIS EXAMINATION RESULT FORM	ii
ACKNOWLEDGEMENTS	iii
ABSTRACT.....	iv
ÖZ	v
LIST OF FIGURES	viii
LIST OF TABLES	xi
CHAPTER ONE – INTRODUCTION	1
CHAPTER TWO – BACKGROUND	6
2.1 Definition of Antenna.....	6
2.1.1 Input Impedance, Voltage Standing Wave Ratio (VSWR) and Return Loss (RL).....	7
2.1.2 Bandwidth.....	10
2.1.3 Directivity and Gain	11
2.1.4 Polarization	13
2.1.5 Fields and Power Radiated by an Antenna	14
2.1.6 Radiation Pattern	16
2.2 Types of Antennas.....	19
2.3 The Techniques to Obtain Wide Operating Bandwidth	20
2.4 Microstrip Antennas	21
2.4.1 Introduction to the Microstrip Antenna	22
2.5 Method of Analysis	26
2.5.1 Finite Difference Time Domain (FDTD) Method and Difference between FDTD and Finite Integration Technique (FIT) Methods.....	28
2.6 CST Microwave Studio	30
2.7 Anechoic Chamber	31

CHAPTER THREE - THE DESIGN OF THE ANTENNAS AND RESULTS . 34

3.1 Specifications of the Antennas and Methodology..... 34
3.2 Measurement Process 36
3.3 The Realization of the Printed Planar Monopole Antennas 39
3.4 Log Periodic Dipole Array Antenna 53
3.5 Koch Fractal Log Periodic Dipole Array Antenna..... 65

CHAPTER FOUR – COUNCLUSION AND FUTURE WORKS 67

REFERENCES..... 70

LIST OF FIGURES

	Page
Figure 2.1 Antenna as a transition device	7
Figure 2.2 Equivalent circuit model for an antenna	8
Figure 2.3 Measurement of the bandwidth (4:1 GHz) from the plot of the reflection coefficient modeled in CST Microwave Studio	11
Figure 2.4 Equivalent circuit of the antenna	12
Figure 2.5 Field regions around an antenna	14
Figure 2.6 Far-field plane wave approximation	16
Figure 2.7 Simulated 3D radiation pattern. Modeled in CST MWS	17
Figure 2.8 2D radiation plot in CST: gain versus θ by keeping $\phi = 0^\circ$	18
Figure 2.9 Radiation pattern of a directional antenna	18
Figure 2.10 Basic structure of a microstrip patch antenna	22
Figure 2.11 Examples for applications of microstrip antennas (a) RFID tag antenna, (b) microstrip phased array antennas for mobile satellite communications	24
Figure 2.12 Types of microstrip antennas (a) printed slot antenna, (b) printed dipole antenna, (c) travelling wave antenna	24
Figure 2.13 Types of feeding methods (a) microstrip line feed, (b) probe feed, (c) aperture-coupled feed, (d) proximity-coupled feed	26
Figure 2.14 Classification of full wave methods	27
Figure 2.15 Embedding of an antenna structure of an antenna in an FDTD	28
Figure 2.16 RF anechoic chamber (a) inner view, (b) closed view	33
Figure 3.1 Flow chart for design methodology	35
Figure 3.2 Anritsu MS4642A VNA	37
Figure 3.3 Basic shape of printed planar monopole antenna	40
Figure 3.4 Geometry of the printed circular disc planar monopole antenna	41
Figure 3.5 The printed circular disc planar monopole antenna. Modeled in CST MWS (a) top view, (b) bottom view	42
Figure 3.6 Realization of the printed circular disc planar monopole antenna (a) top view, (b) bottom view	43

Figure 3.7	Comparison of measured and simulated S_{11} for the printed circular disc planar monopole antenna (--- measurement, — simulation)	43
Figure 3.8	Measured and simulated E-plane polar radiation patterns of the circular disc printed planar monopole antenna (--- measurement, — simulation) (a) 1 GHz, (b) 1.5 GHz, (c) 2 GHz	44
Figure 3.9	Measured and simulated H-plane polar radiation pattern of the circular disc printed planar monopole antenna (--- measurement, — simulation) at (a) 1 GHz, (b) 1.5 GHz, (c) 2 GHz	45
Figure 3.10	Configuration position of the patches in the SCFC method	47
Figure 3.11	Geometry of the broadband modified rectangular planar monopole antenna. Modeled in CST Microwave Studio (a) top view, (b) forward view	49
Figure 3.12	Realization of the broadband modified rectangular planar monopole antenna (a) top view, (b) bottom view	50
Figure 3.13	Simulation and measurement S_{11} of the broadband modified rectangular monopole antenna (--- measurement, — simulation)	50
Figure 3.14	Measured and simulated E-plane polar radiation pattern of modified rectangular printed planar monopole (--- measurement, — simulation) at (a) 1 GHz, (b) 1.5 GHz, (c) 2 GHz	51
Figure 3.15	Measured and simulated H-plane polar radiation pattern of modified rectangular printed planar monopole (--- measurement, — simulation) at (a) 1 GHz, (b) 1.5 GHz, (c) 2 GHz	52
Figure 3.16	Log periodic dipole array	54
Figure 3.17	Log periodic array associated connections. (a) straight line, (b) crisscross	55
Figure 3.18	Computed contour of constant directivity versus σ and τ for log periodic dipole arrays	57
Figure 3.19	Relative characteristic impedance of a feeder line as a function of relative characteristic impedance of dipole element	59
Figure 3.20	Printed log periodic dipole array antenna. (a) modeled in CST Microwave Studio, (b) realization of the antenna	61

Figure 3.21	Printed log periodic dipole array antenna (a) modeled in CST Microwave Studio, (b) realization of the antenna.....	61
Figure 3.22	Measured and simulated E-plane polar radiation pattern of PLPDA (--- measurement, — simulation) at (a) 1 GHz, (b) 1.5 GHz, (c) 2 GHz, (d) 2.5 GHz, (e) 3 GHz.....	63
Figure 3.23	Measured and simulated H-plane polar radiation pattern of PLPDA (--- measurement, — simulation) at (a) 1 GHz, (b) 1.5 GHz, (c) 2 GHz, (d) 2.5 GHz, (e) 3 GHz.....	64
Figure 3.24	Koch-Fractal Log-Periodic Antenna (a) geometry, (b) realization.....	65
Figure 3.25	Simulation results of KFLPA (a) simulated return loss, simulated E-Plane and H-plane polar radiation patterns at (b) 1 GHz, (c) 1.5 GHz, (d) 2 GHz, (e) 2.5 GHz (--- E-Plane, — H-Plane), (f) maximum gain over frequency	66

LIST OF TABLES

	Page
Table 2.1	Broadband techniques for some kind of microstrip antennas..... 21
Table 2.2	Some of the electromagnetic simulation programs to their numerical solving technique 28
Table 3.1	Optimal design parameters for the printed circular patch monopole antenna..... 42
Table 3.2	Calculated and simulated broadside gains for different frequencies for printed circular disc monopole antenna 44
Table 3.3	Design parameters for broadband modified rectangular monopole antenna..... 50
Table 3.4	Calculated and simulated broadside gains for different frequencies for broadband modified rectangular monopole antenna..... 51
Table 3.5	Design parameters for PLPDA 60
Table 3.6	PLPDA dimensions (1 is the longest dipole 17 is the shortest dipole .. 60
Table 3.7	Calculated and simulated broadside gains for different frequencies for PLPDA..... 62

CHAPTER ONE

INTRODUCTION

Transfer of information between at least two points can be done using sound, infrared, optical or radio frequency energy. By wireless communication, this process can be done without direct connection. Today, majority of wireless systems uses radio frequency or microwave signals, mostly in UHF to millimeter wave frequency range. Higher frequencies are desired due to crowded spectrum at low frequencies and requirement for higher data rate. Today most of the wireless systems work at frequency ranging from several Megahertz (MHz) to several Gigahertz (GHz) (Pozar, 2012). Some of the applications of wireless systems include Global Positioning System (GPS), Wireless Fidelity (Wi-Fi), Global System for Mobile Communication (GSM), The Third Generation of mobile Telecommunications Technology (3G), and Long Term Evaluation (LTE) systems. Due to these wide application areas, the importance of wireless communication is increasing day by day.

An antenna, which works at the operating frequency of the system, is an important component of any wireless communication system. Furthermore, many antenna performance parameters such as return loss, operation bandwidth, radiation pattern and gain must be fulfilled with admissible dimensions in wireless communication systems (Bozdağ, 2014; Waterhouse & Novak, 2007; Hassanien & Hamad, 2010).

There is wide variety of antennas. One of them is microstrip antenna. This type of antenna has become attractive. Because, they are inexpensive and also robust, they are used in many communication systems. However, they have narrow bandwidth, which is one of the disadvantages. Due to the fact that many devices such as cellular phone and tablets need to operate different frequency bands, the antennas used in these devices should be either wideband or multi-band (Bozdağ, 2014; Balanis, 2005; Ávila-Navarro & Reig, 2012; Tamaoka, Hamada & Ueno, 2004; Koyya, Valluri &

Raju, 2013). At this thesis, the solution is concentrated on the design of an antenna working in a wide frequency range.

In this study, planar monopole antennas and a log periodic dipole array (LPDA) antenna are simulated and manufactured. In addition to their wideband characteristics, the other reason for the concentration on is, monopole antennas and especially log-periodic antennas can be used in anechoic chambers (Morgan, 2007). Microstrip log periodic dipole antennas are implemented to the anechoic chamber, which is located on Antenna and Microwave Technique Laboratory of Dokuz Eylül University. The operating frequency of the antennas is from 750 MHz to 3000 MHz. The first planar monopole antenna is based on circular disc. The second planar monopole antenna is based on modified rectangular shape by using stepped cut at four corners method and T-shaped slot (Moradikordalivand, Rahman, Ebrahimi & Hakimi, 2014; Chaiteang, Ghankaew, Chareonsiri & Thaiwirot, 2014). Then, a printed log periodic dipole array is designed by the help of standard log periodic dipole array antenna formulations with some modifications (Carrel, 1961; Balanis, 2005; Pozar, 2012). Also, Koch Fractal log periodic dipole array antenna is designed.

These antennas are simulated by using Computer Simulation Technology (CST) Microwave Studio (MWS) and manufactured on both side of the FR4 dielectric substrate by using printed circuit techniques. Manufactured antennas are measured in the Dokuz Eylül University Antennas and Microwave Technique Laboratory. Simulation and measurement results show that the operating frequency of each antenna is almost from 750 MHz to 3000 MHz, and planar monopole antennas have nearly omni-directional radiation patterns, while log-periodic dipole array antennas have directional radiation patterns.

This thesis is organized in four chapters.

The following section of this chapter gives the motivation of the study.

In Chapter 2, the background of the thesis work is given by including antenna theory, brief introduction of microstrip antennas, information about numerical method and CST. In this chapter, a short explanation about anechoic chambers is also described.

In Chapter 3, specifications of the and methodology of the wideband antennas are mentioned in detail. The measurement process is explained, planar monopole and log periodic dipole array antennas are given briefly. Furthermore, simulation and measurement results are demonstrated by graphs and figures.

In Chapter 4, the conclusion of the thesis is given.

The motivation of the thesis is given in the next seven paragraphs.

Most of the wireless systems have their own operating frequency bands. Therefore, many devices such as cellular phone or tablets operate at different frequency bands. At this point, one of the solution is to design an antenna working at wide frequency ranges (Mondal & Sarkar, 2014; Lee, Huang, Yang & Wang, 2008). Today, GPS, Wi-Fi, GSM, 3G, LTE are some applications of wireless systems, which are explained in the following part of the chapter. The manufactured antennas in the thesis are fully or partially suitable with these systems.

GPS, which is acronyms of “The Global Positioning Satellite System”, was originally developed by the military. GPS is used to determine an accurate position on Earth either on land or in air or at sea. The position information includes latitude, longitude and elevation data for the users. GPS utilizes 24 satellites in medium Earth orbits to provide this information. As mentioned in Pozar’s work in (2001), GPS was originally developed as NAVSTAR system by the military at a cost of about \$12B. It now becomes most commonly used worldwide wireless technology for business purposes.

GPS, functions with two separate frequency bands to transmit spread spectrum signals: L1 at 1575.42 MHz which transmits ephemeris data for each satellite and timing codes. L2 at 1227.60 MHz which uses an encrypted timing code referred to as the Protected (P) code (there is also a P code signal transmitted at the L1 frequency). While L1 is mostly available to any commercial and public users, which is also referred to as the Course/Acquisition (C/A) code, on the other hand L2 frequency is reserved only for military use (Pozar, 2001).

As it has been described by University of California, Irvine Environmental Health & Safety; Radiation Safety Division (2008), “Wireless Fidelity” which is referred as “Wi-Fi” is the commercial name of WLAN. “Wi-Fi” is basically a wireless network that provides communication for computers through radio frequency radiation similar to cell phones or two way radios (walkie-talkies). Wi-Fi utilizes protocols of Institute of Electrical and Electronics Engineers (IEEE) 802.11 and locates different radio frequency spectrum such as 2.4 GHz, 3.6 GHz, 4.9 GHz and 5 GHz band (Bozdağ, 2014).

A globally accepted standard for digital cellular communication GSM which is acronym for Global System for Mobile Communication is the name of a standardization group established in 1982. The aim is to create a common European mobile telephone standard. As The International Engineering Consortium [IEC] (n.d), mentions this standard to formulate specifications for a pan-European mobile cellular radio system operating at 900 MHz, and also adds that many countries outside of Europe will join the GSM partnership.

International Mobile Telecommunications- 2000 is the set of standards for the third generation of mobile telecommunications technology (3G). The advanced services and applications such as voice telephony, mobile internet access, mobile television and video calling are all provided by 3G, which creates higher capacity and network functionalities. Although 2100 MHz band is mainly used for 3G applications by the all service providers in Turkey, IMT-2000 frequency allocation is not standard among the other countries. The range of different frequency bands from

450 MHz to 3600 MHz are used in different countries around the world (International Telecommunication Union [ITU], 2003; Bozdağ, 2014).

In 2007, Long Term Evolution (LTE) was considered a future development in cellular 3G services. It is now providing several technical advantages to the cellular networks. LTE is a 3GPP standard, which allows different uplink and downlink speeds. While uplink speed is up to 50 megabits per second (Mbps), the downlink speed is up to 100 Mbps. The wide scope of scale between 1.25 MHz to 20 MHz has several benefits such that, it will fulfill the requirement of the various bandwidth allocations for different network operators, and operators will be adequate to provide range of services based on spectrum (Zyren, 2007). One of the popular LTE band is at 2.6 GHz (Curwen & Whalley, 2013).

CHAPTER TWO

BACKGROUND

The main purpose of this study is to design antennas, which are convenient for the desired frequency range. In this chapter, the fundamental antenna theory is given, and some important parameters of antennas are described. Types of antennas and some requirements about wide operating bandwidth of the antenna are also explained. Following parts of the chapter, short introduction of microstrip antennas, explanation about numerical method and CST Studio are given. Also, in this chapter, a short explanation about anechoic chambers is described and small-size rf anechoic chamber, which is located in Dokuz Eylül University Antenna and Microwave Technique Laboratory is shown.

2.1 Definition of Antenna

The IEEE defines an antenna as “that part of a transmitting or receiving system that is designed to radiate or to receive electromagnetic waves” (Stutzman & Thiele, 2013). Moreover, a transit antenna is a device that converts signals which are conveyed from a transmission line into electromagnetic waves and then radiate them into free space (Liang, 2006) as shown in Figure 2.1.

Transmission line which is shown in Figure 2.1, is used to transmit electromagnetic energy from the transmitting source to the antenna or from antenna to the receiver. Coaxial line, waveguide and microstrip line are some types of transmission line (Balanis, 2005).

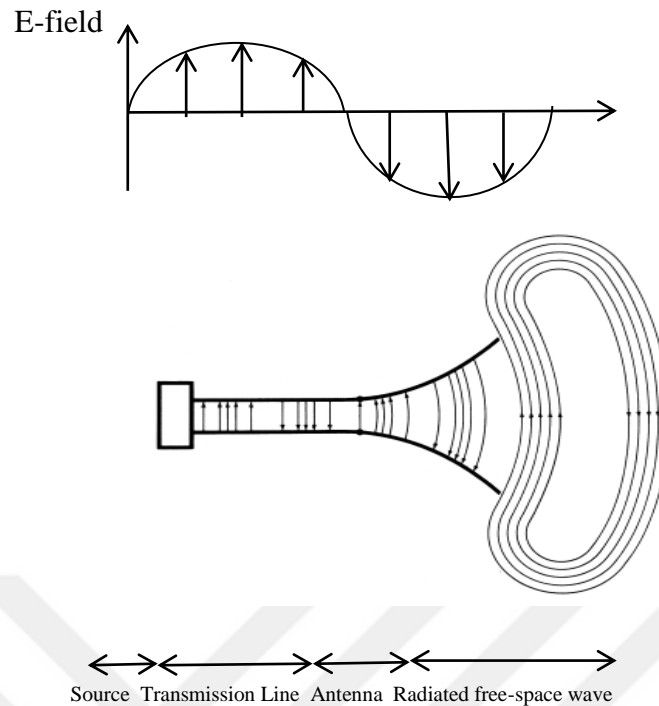


Figure 2.1 Antenna as a transition device (Balanis, 2005)

Liang (2006), emphasizes the necessity of defining the various parameters in order to describe the performance of an antenna and describes a number of widely used antenna parameters which are applicable such as bandwidth, radiation pattern, gain, input impedance, and so on. Some of these parameters are explained as follows.

2.1.1 Input Impedance, Voltage Standing Wave Ratio (VSWR) and Return Loss (RL)

Input impedance is defined in Balanis (2005), as ‘The impedance presented by an antenna at its terminals or the ratio of voltage to the current at the pair of terminals or the ratio of the appropriate components of the electric to magnetic fields at a point.’

Other components or antennas can affect the input impedance of an antenna (or simply antenna impedance). However, the given formulas below are for an isolated antenna. Antenna impedance includes real and imaginary parts such that (Stutzman & Thiele, 2013).

$$Z_A = R_A + j X_A \quad (2.1)$$

where, Z_A is antenna impedance at the terminals, R_A is antenna resistance at the terminals, X_A is antenna reactance at the terminals. V_s is source voltage.

The equivalent circuit model for an antenna is shown in Figure 2.2.

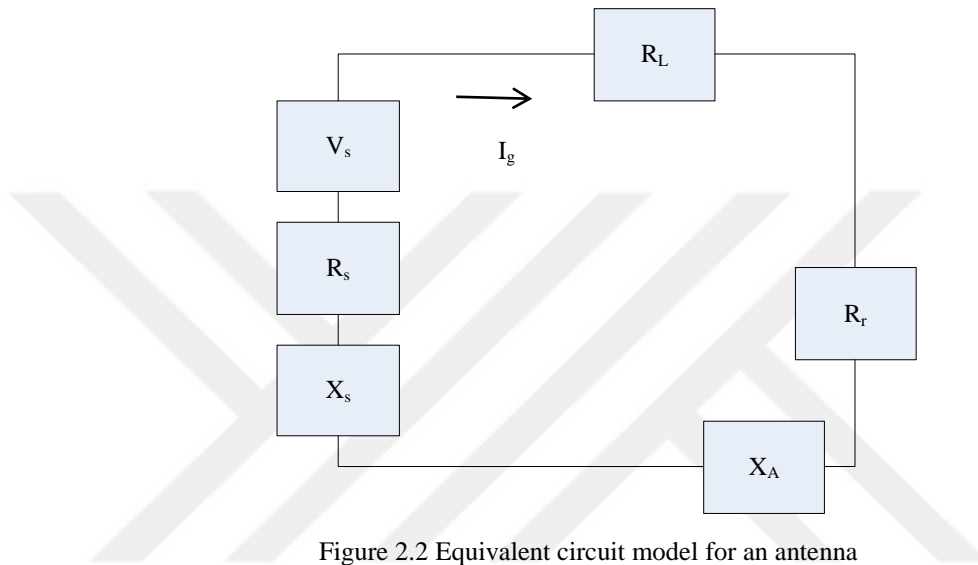


Figure 2.2 Equivalent circuit model for an antenna

By considering Figure 2.2, antenna resistance is described as

$$R_A = R_r + R_L \quad (2.2)$$

where, R_r is radiation resistance of the antenna, R_L is loss resistance of the antenna.

There are two parts of the antenna impedance, which are the imaginary part and the resistive part. The imaginary part X_A indicates the stored power in the adjacent field to the antenna. The resistive part R_A consists of two parts the radiation resistance R_r and the loss resistance R_L . The power radiated by the antenna is actually the power incorporated with the radiation resistance. The emitted heat time, equivalently the power dissipated in the loss resistance, is caused by the antenna itself due to dielectric or conducting losses (Nakar, 2004).

Impedance of the source (Z_S) is given as:

$$Z_S = R_S + j X_S \quad (2.3)$$

where, R_S is resistance of the source, and X_S is reactance of the source.

The full transfer of power, which occurs specifically when the impedance of the antenna (Z_A) is compatible to the impedance of the source (Z_S), is required between the transmitter and the antenna to allow the antenna to function efficiently.

The maximum power transfer theorem states that the maximum transferred power can be achieved if and only the impedance of the transmitter is a complex conjugate of the impedance of the antenna under consideration or other way around.

$$Z_A = Z_S^* \quad (2.4)$$

When this condition is not satisfied, standing waves are created. This is because some of the power might be reflected back. Voltage Standing Wave Ratio (VSWR) is a parameter can directly related with standing waves. The mismatch between the antenna and the transmitter can be observed by checking VSWR. The higher VSWR represent greater mismatch (Nakar, 2004).

$$VSWR = \frac{1 + |\Gamma|}{1 - |\Gamma|} \quad (2.5)$$

where;

$$\Gamma = \frac{Z_A - Z_S}{Z_A + Z_S} \quad (2.6)$$

where, Γ is called as reflection coefficient.

For practical applications, the maximum acceptable value of VSWR is usually 2 (Chen & Chia, 2006).

Return Loss (RL), which is a kind of loss, occurs when antenna and source are mismatched. Then, all available power from the generator can not be delivered to the antenna.

$$RL(\text{dB}) = -20\log |\Gamma| \text{ dB} \quad (2.7)$$

Here, $\Gamma = 0$ ($RL = \infty$ dB) means source and antenna are matched (No reflected power), whereas a $\Gamma = 1$ ($RL = 0$ dB) means all incident power is reflected.

For practical applications, 10 dB return loss is acceptable (Chen & Chia, 2006).

2.1.2 Bandwidth

The definition of the bandwidth of an antenna is given in Balanis (2005), as ‘the range of frequencies within which the performance of the antenna, with respect to some characteristic, conforms to a specified standard.’ The bandwidth is related with maximum and minimum frequencies around a center frequency at which the antenna characteristics such as input impedance, pattern, beamwidth and radiation efficiency satisfy acceptable value of those at frequency. The ratio of the upper-to-lower frequencies is generally gives the bandwidth of the broadband antennas (having more than 3:1 bandwidth). Also, a percentage of the frequency difference (upper minus lower) over the center frequency of the bandwidth usually gives the bandwidth of the narrowband antennas (Balanis, 2005).

$$BW_b = \frac{f_u}{f_L} \text{ (for broadband antennas).} \quad (2.8)$$

$$BW_n = f_u - f_L, BW_n(\%) = \frac{f_u - f_L}{f_c} \times 100 \text{ (for narrowband antennas).} \quad (2.9)$$

where, BW_b = broadband bandwidth, BW_n = narrowband frequency bandwidth, $BW_n(\%)$ = narrowband percentage bandwidth, f_u = upper frequency, f_L = lower frequency, and f_c = center frequency.

In Figure 2.3, bandwidth (4:1) of a broadband antenna respect to S_{11} (dB) parameter is shown, between 0.3 and 4 GHz frequency band.

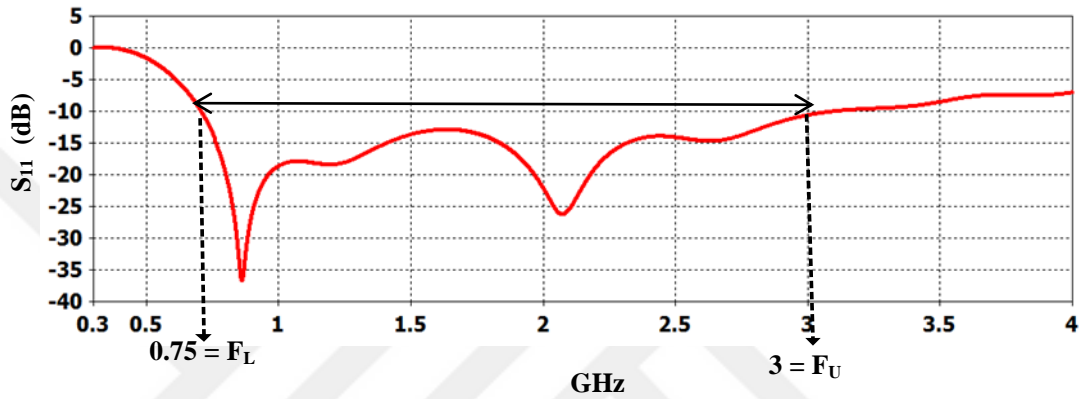


Figure 2.3 Measurement of the bandwidth (4:1) from the plot of the reflection coefficient. Modeled in CST Microwave Studio

2.1.3 Directivity and Gain

The directional properties of the antenna radiation pattern can be described with two inputs, the introduction of the directivity D and definition of the ratio which belongs to the radiation intensity U in a given direction from the antenna over that of an isotropic source. For an isotropic source, the radiation intensity U_0 is equal to the total radiated power P_{rad} divided by 4π (Liang, 2006). Directivity D can be calculated by the following formula:

$$D = \frac{U}{U_0} = \frac{4\pi U}{P_{rad}} \quad (2.10)$$

By using following formula maximum directivity can be calculated when the direction is not specified.

$$D_{max} = \frac{U_{max}}{U_0} = \frac{4\pi U_{max}}{P_{rad}} \quad (2.11)$$

where D_{max} is the maximum directivity, and U_{max} is the maximum radiation intensity.

Directivity, which is the ratio of two radiation intensities are given in (2.11), is a dimensionless quantity, and it is typically expressed in dBi. The radiation pattern of the antenna provides an easy estimation for the directivity of an antenna. The width of the main lobe defines the quality of the directivity of an antenna. While a narrow main lobe provides a better directivity, the directivity is lower for a broad main lobe (Nakar, 2004).

Antenna gain (G) is directly concerned with the directivity. On the other hand, it considers the radiation efficiency e_{rad} of the antenna, and characteristics is given by;

$$G = e_{rad}D \quad (2.12)$$

Figure 2.4. shows the equivalent circuit of the antenna, where R_r , R_L , L and C represent the radiation resistance, loss resistance, inductor and capacitor, respectively.

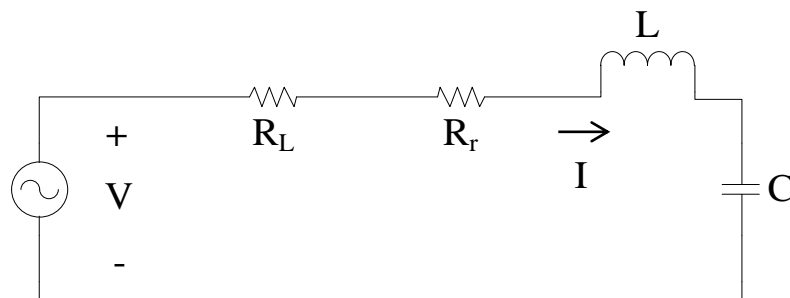


Figure 2.4 Equivalent circuit of the antenna

The ratio of the power delivered to the R_r to the power delivered to R_r and R_L describes e_{rad} . Therefore, the radiation efficiency e_{rad} can be written as

$$e_{rad} = \frac{\frac{1}{2} |I|^2 R_r}{\frac{1}{2} |I|^2 R_r + \frac{1}{2} |I|^2 R_L} = \frac{R_r}{R_r + R_L} \quad (2.13)$$

The maximum gain (G_{max}) is concerned with the maximum directivity D_{max} given in following equation (Liang, 2006):

$$G_{max} = e_{rad} D_{max} \quad (2.14)$$

2.1.4 Polarization

The polarization of the radiated wave can be described specification of an electromagnetic wave characterize the time-varying direction and relative magnitude of the electric-field vector. The antenna polarization is expressed by the polarization of the wave radiated in a given direction by the antenna when in transmitting mode. If direction is not defined, the polarization in the direction of maximum gain is taken (Balanis, 2005; Stutzman & Thiele, 2013).

The most common types of polarizations are linear including horizontal and vertical, circular and elliptical including right hand polarization and left hand polarization (Balanis, 2005).

The electric field vector is linearly polarized when it is back and forth a long line. On the other hand, the electric field vector keeps constant in length but rotates around circular path in a circularly polarized wave. By considering that it is locked the wave from behind of the propagation when the wave rotates around counter clockwise it is called a left hand circular polarized and when the motion is opposite to this which is clockwise motion, it is called right hand circular polarized (Nakar, 2004).

2.1.5 Fields and Power Radiated by an Antenna

Reactive near-field region, radiating near-field region, and far-field region are three regions respect to area covering an antenna as given in Figure 2.5. This is because, the field patterns of an antenna vary with distance, and are related with radiating energy and reactive energy (Balanis, 2005).

Moreover, the area surrounding an antenna can be separated into three regions. They are reactive near-field region, radiating near-field region, and far-field region.

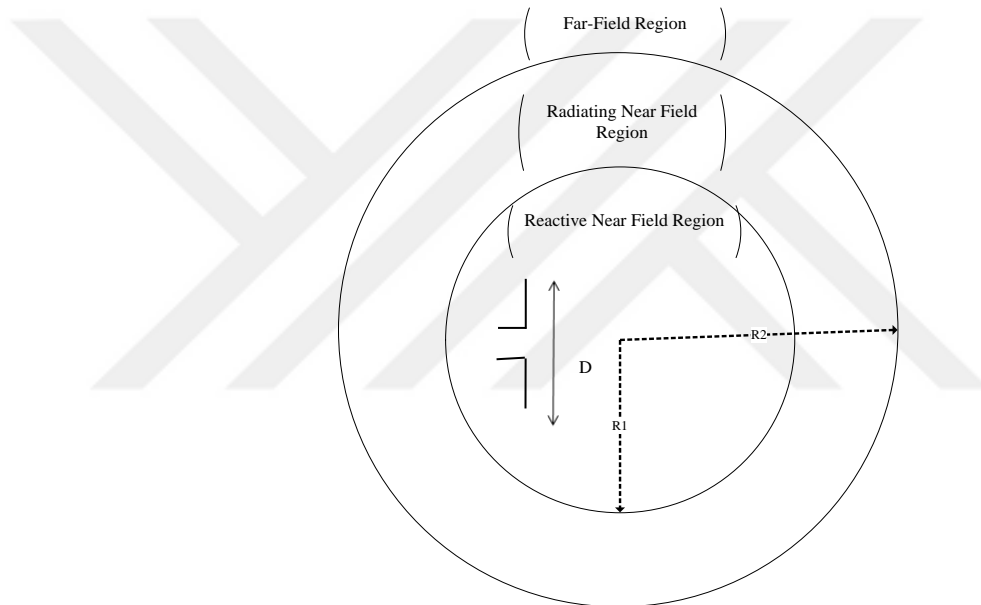


Figure 2.5 Field regions around an antenna

Reactive near-field region: In this region, the reactive field predominates and it is the first region surround the antenna. In this region, energy is stored and not distributed. The distance of the outermost border for this region is calculated as

$$R_1 = 0.62 \sqrt{D^3 / \lambda} \quad (2.15)$$

where R_1 is the distance from the antenna surface, D is the largest dimension of the antenna and λ is the wavelength.

Radiating near-field region (Fresnel region): This is the region which, take place between the reactive near-field region and the far field region. In this region, radiation field predominate and there is a relation between the angular field distribution and the distance from the antenna. The outer border is at a distance:

$$R_2 = 2D^2/\lambda \quad (2.16)$$

where R_2 is the distance from the antenna surface which is also known as the most commonly used far-field condition (Balanis, 2005).

Far-field region (far-zone region): Spherical shape wave radiate by a point source, with the wavefront widening outward at a rate equal to the phase velocity (u_p) (if the medium is free space then, $u_p = c$). If the distance between the transmitting antenna and the receiving antenna (R), is large enough that the wavefront reaches the receiving aperture, is expressed to be in the far-field (or far-zone) region of the transmitting point source. In this region, there is no relation between angular field distribution and the distance from the antenna (Ulaby, 2007; Balanis, 2005). Figure 2.6 shows far-field plane wave approximation.

The localized near-zone fields are negligible at sufficiently long distance. Equation 2.17 gives the radiated electric field of an arbitrary antenna.

$$\overline{E}(r, \theta, \varphi) = [\hat{a}_\theta F_\theta(\theta, \varphi) + \hat{a}_\phi F_\phi(\theta, \varphi)] \frac{e^{-jk_0 r}}{r} \text{ V/m} \quad (2.17)$$

where, \overline{E} demonstrates the electric field vector, \hat{a}_θ and \hat{a}_ϕ are unit vectors in the spherical coordinate system, r shows the radial distance from the origin, and $k_0 = 2\pi/\lambda$ is the free-space propagation constant, wavelength (λ) = c/f . Furthermore, described in (2.17) $F_\theta(\theta, \varphi)$ and $F_\phi(\theta, \varphi)$, are the pattern functions The explanation of (2.17) is that this electric field propagates in the radial direction with a phase variation of $e^{-jk_0 r}$, and an amplitude variation with distance of $1/r$. Direction of the

polarization of the electric field can be either the \hat{a}_θ or \hat{a}_ϕ . Due to this is a TEM wave, not in the radial direction (Pozar, 2012).

Following formulas show the magnetic field associated with the electric field as

$$H_\phi = \frac{E_\theta}{\eta_0} \quad (2.18)$$

$$H_\theta = \frac{-E_\phi}{\eta_0} \quad (2.19)$$

where η_0 is the wave impedance of free-space, equal to 377 Ω .

Transverse directions are only directions that the magnetic field vector is polarized. The Poynting vector for this wave is:

$$\bar{S} = (\bar{E} \times \bar{H}^*) \text{ W/m}^2 \quad (2.20)$$

Time average Poynting vector is (Pozar, 2012):

$$\bar{S}_{\text{avg}} = \frac{1}{2} \text{Re}\{\bar{S}\} = \frac{1}{2} \text{Re}\{\bar{E} \times \bar{H}^*\} \text{ W/m}^2 \quad (2.21)$$

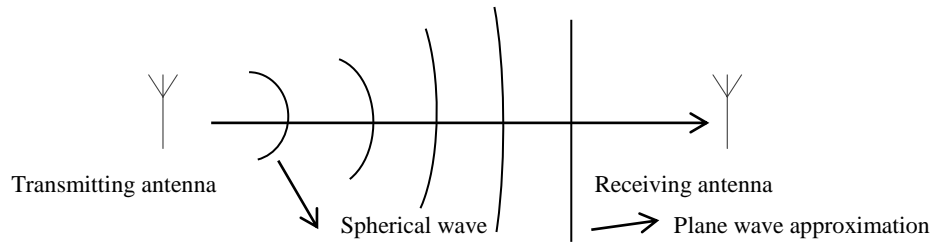


Figure 2.6 Far-field plane wave approximations

2.1.6 Radiation Pattern

The radiation pattern of an antenna is a graphical representation of power distribution of field strength of the antenna as a function of the spatial co-ordinates,

which are usually defined by elevation angle θ and the azimuth angle ϕ of spherical coordinate system. Three dimensional (3D) graph and polar plot are two of them (Seçmen, 2011).

To measure the three dimensional radiation patterns, a spherical coordinate system is used. Spherical coordinate system describes relative strength of radiation power in the far field for a sphere covering the antenna. Figure 2.7 shows simulated 3D radiation pattern in CST Microwave Studio. Here x-z plane, which is one of the plane of the spherical coordinate system, generally describes the elevation plane (theta). For this specific example, it is also E-plane which includes the electric-field vector and the direction of maximum radiation. The x-y plane, which is the other plane of the spherical coordinate system, describes the azimuth plane (phi). Again, for the pattern in Figure 2.7, it is H-plane and which includes the direction of maximum radiation. Polar plot by keeping one of the variables of ϕ (phi) or θ (theta) and changing the other presents a two-dimensional radiation pattern (Powell, 2001). Figure 2.8 shows a sample two dimensional radiation plot which contains a varying θ , and $\phi = 0^\circ$.

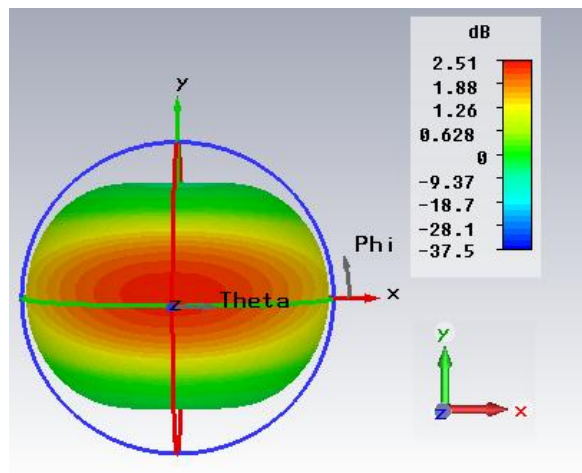


Figure 2.7 Simulated 3D radiation pattern. Modeled in CST Microwave Studio

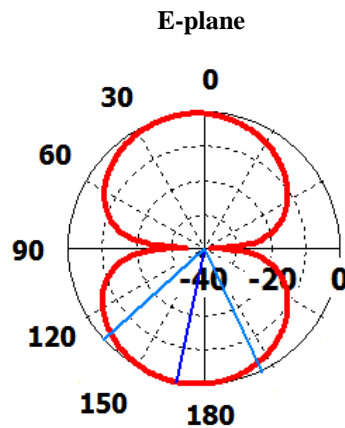


Figure 2.8 2D radiation plot in CST: gain versus θ by keeping $\phi = 0^\circ$

There are three common types of radiation patterns:

- (a) Isotropic - A hypothetical lossless antenna radiate electromagnetic waves equally in all directions. It is just acceptable for an ideal antenna. The directive properties of actual antennas can be expressed with reference to this ideal antenna.
- (b) Directional - In some directions electromagnetic waves radiate or receive more effectively than the other directions.
- (c) Omni-directional – These antennas have non-directional pattern in a given plane and they have directional plane in any orthogonal plane (Balanis, 2005).

The radiation pattern plot of a directional antenna is given in Figure 2.9.

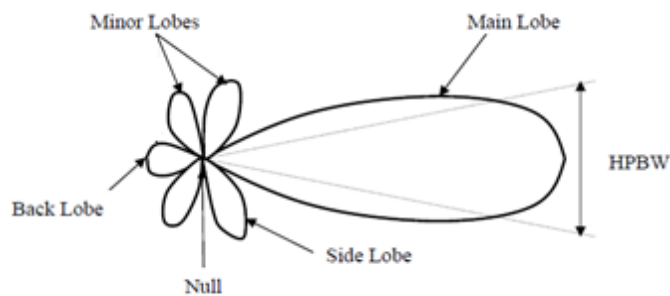


Figure 2.9 Radiation pattern of a directional antenna (Nakar, 2004)

- **HPBW:** The half power beamwidth (HPBW) can be described as the angle subtended by the half power ($0.5 P_{\max}$) points of the main beam.
- **Main Lobe:** This is lobe at the direction of maximum radiation.
- **Minor lobes:** Minor lobes are the name of all the lobes except the minor lobes. These lobes show the radiation in unwanted directions.
- **Back Lobe:** This is the minor lobe and occurred opposite position of the main lobe
- **Side Lobe:** These is a kind of minor lobe which is contiguous to the main lobe and it is distinguished between each other by various nulls. Side lobe is generally one of the largest minor lobes.

Generally, a good antenna design has minimal minor lobes in most wireless systems. This is because, minor lobes are not usually desired (Nakar, 2004).

2.2 Types of Antennas

Many applications need an antenna, for this purpose various antennas have been proposed. According to Pozar (2012), they can be categorized as follow:

- **Wire antennas** mostly have low gains, usually suitable with lower frequencies (HF to UHF), have some advantages such as being cheap, having light duty and can be designed easily. Dipoles, monopoles, loops, sleeve dipoles are some examples of wire antennas.
- **Aperture antennas** generally convenient for microwave and millimeter wave frequencies have moderate to high gains. Open-ended waveguide, rectangular or circular horns, reflectors, lenses are some kinds of aperture antennas.

- **Printed antennas** generally are used at microwave and millimeter wave frequencies, high gains can be obtained. Printed slots, printed dipoles, and microstrip patch antennas are some examples of printed antennas. Radiating elements and associated feed circuitary are realized on dielectric substrates.
- **Array antennas** are occurred organized arrangement of multiple antennas with a feed network. Side lobe levels, beam pointing angle and other pattern characteristics are available to control by setting the amplitude and phase excitation of the array elements.

2.3 The Techniques to Obtain Wide Operating Bandwidth

Narrowband, intermediate band, and wideband are three qualitative groups, which classify the response of each antenna with respect to frequency (Balanis, 2005).

An antenna is a general requirement for many system applications in order to operate over a wide range of frequencies. Wideband antenna, which is a generic name for an antenna with wide bandwidth, is referred as a broadband antenna (Stutzman & Tiele, 2013).

Chen & Chia (2006), categorized wideband techniques for some of the microstrip antennas under three approaches. Table 2.1 summarizes them as given below.

Table 2.1 Broadband techniques for some kind of microstrip antennas

Approach	Techniques
Lower the Q (Quality factor)	Select the radiator shape
	Thicken the substrate
	Lower the dielectric constant
	Increase the losses
Use impedance matching	Insert a matching network
	Add tuning elements
	Use slotting and notching patches
Introduce multiple resonances	Use parasitic (stacked or co-planar) elements
	Use slotting patches, insert impedance networks
	Use an aperture, proximity coupling

According to Balanis (2005), total quality factor “Q” of an antenna is inversely proportional to the fractional bandwidth of the antenna (FBW).”

$$FBW = \frac{1}{Q} \quad (2.23)$$

“FBW is given as the percentage of the frequency difference over the center frequency” (Liang, 2006).

$$FBW = 2 \frac{f_U - f_L}{f_U + f_L} \quad (2.24)$$

In this thesis, “select the radiator shape” technique under the lower the quality factor (Q) approach has been used for the printed planar monopole antennas.

2.4 Microstrip Antennas

In this thesis, due to their advantages such as low weight, low volume and low fabrication cost, the microstrip antennas are preferred.

In this part of the chapter the introduction to the microstrip antenna, their advantages and disadvantages, types, some examples of the application areas and some feed modeling techniques are given.

2.4.1 Introduction to the Microstrip Antenna

Basically, a microstrip antenna consists of a metallic patch (radiated patch) printed on top of a dielectric substrate, which has a ground plane on the bottom of the dielectric substrate as shown in Figure 2.10. Metallic patch made of a conducting material (copper or gold in general) can be any shape.

Various types of substrate can be used with their dielectric constants (ϵ_r) in the range of $2.2 \leq \epsilon_r \leq 12$ for the design of microstrip antennas (Balanis, 2005).

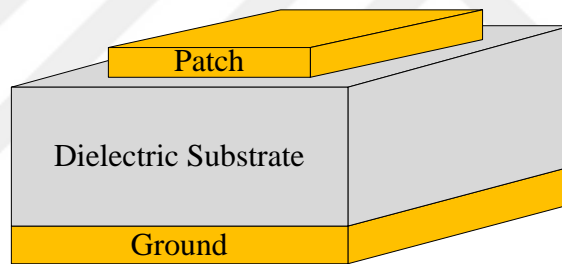


Figure 2.10 Basic structure of a microstrip patch antenna

Microstrip antennas have several advantages. These are discussed in Balanis (2005), and therefore many applications cover the broad frequency range from 100 MHz to 100 GHz (Garg, Bhartia, Bahl & Ittipiboon, 2001). The Advantages of the microstrip antennas are:

- Low weight and volume
- Conformability to planar and non-planar surface
- Low fabrication cost

- Allowing simultaneously fabrication of matching networks and feeding lines with antenna structure
- Mechanically robust when mounted on rigid surfaces, compatible with MMIC designs

However, they have also some disadvantages compared to other conventional antennas which are discussed by Balanis (2005), and Garg et al. (2001), such as

- Low efficiency
- Low power
- High Q (sometimes in excess of 100)
- Poor polarization purity
- Very narrow frequency bandwidth
- Lower gain

In 1953, Deschamps proposed the use of microstrip feed lines to feed an array of printed antenna elements, this is accepted as the origin of microstrip antennas. However, the printed antenna elements introduced there were flared planar horn but not microstrip patches. In the early 1970's Howell and Munson performed the first practical implementations of microstrip antennas. The commercial systems began widely adopting Microstrip Antenna beginning from 1990's (Howell, 1972; Munson, 1974; Volakis, 2007; Stutzman & Tiele, 2013).

Researchers and engineers give more importance to microstrip antennas and arrays and these antennas have been used extensively in RF and microwave systems such as communications, radar, navigation, remote sensing, and biomedical systems

(Chen & Chia, 2006). Figure 2.11 gives some example for applications of microstrip antennas.

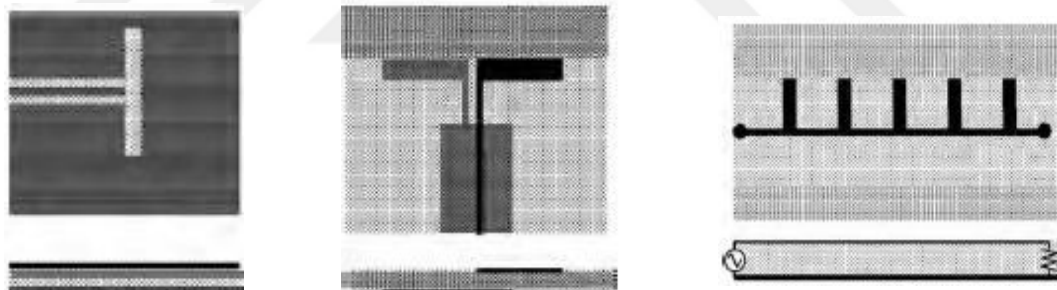


(a)

(b)

Figure 2.11 Examples for applications of microstrip antennas (a) RFID tag antenna (C.F. Huang & Y.F. Huang, 2012), (b) microstrip phased array antennas for mobile satellite communications (Garg et al., 2001)

Microstrip antennas can be in different forms, such as patch, dipole, slot, or a traveling-wave structure, designed for certain applications (Chen & Chia, 2006). In Figure 2.12, types of microstrip antenna are depicted.



(a)

(b)

(c)

Figure 2.12 Types of microstrip antennas (a) printed slot antenna, (b) printed dipole antenna, (c) travelling wave antenna (Chen & Chia, 2006)

After successful application of rectangular patch antennas, printed dipoles become more recognized, although most of the studies have been made on wire dipoles. The width-to-length ratio differentiates the printed patches from dipole antennas. For printed dipole antennas, the radiator width must be less than 0.05 of free space wavelength. Dipole antennas and patch antennas have similar radiation patterns and gain characteristics, their bandwidth are low. For the special reasons, as the printed

dipoles requires less area, they are being used commonly particularly in array antennas. (Garg et al., 2001; Pozar, 1983).

Printed slot antennas, which are composed by subtracting any number and shape of striplines from ground planes of microstrip antennas, are capable to provide dualband or multiband resonant characteristics and circular polarization (Bozdağ, 2014).

A microstrip traveling-wave antenna (MTA), which can be designed so that the main beam lies in any direction from broadside to end fire, may be formed from chain-shaped periodic conductors or a long microstrip line of sufficient width to support a Transverse Electric (TE) mode. To prevent from the standing waves on the antenna, the other end of the traveling wave antenna is terminated with a matched resistive load (Garg et al., 2001).

Usually in microstrip antennas radiating elements exist on one side of the dielectric substrate of microstrip antennas. Earlier, either microstrip line or a coaxial probe fed microstrip antennas through the ground plane. Today, there are more feeding techniques such as coaxial feed, proximity-coupled microstrip feed, aperture coupled microstrip feed (Garg et al., 2001). Impedance matching and geometry of the antenna are directly governed by the design of the feeding structure. The feeding structure is an important factor in widening the impedance bandwidth and enhancing radiation performance (Chen & Chia, 2006). Figure 2.13 shows some types of feeding methods.

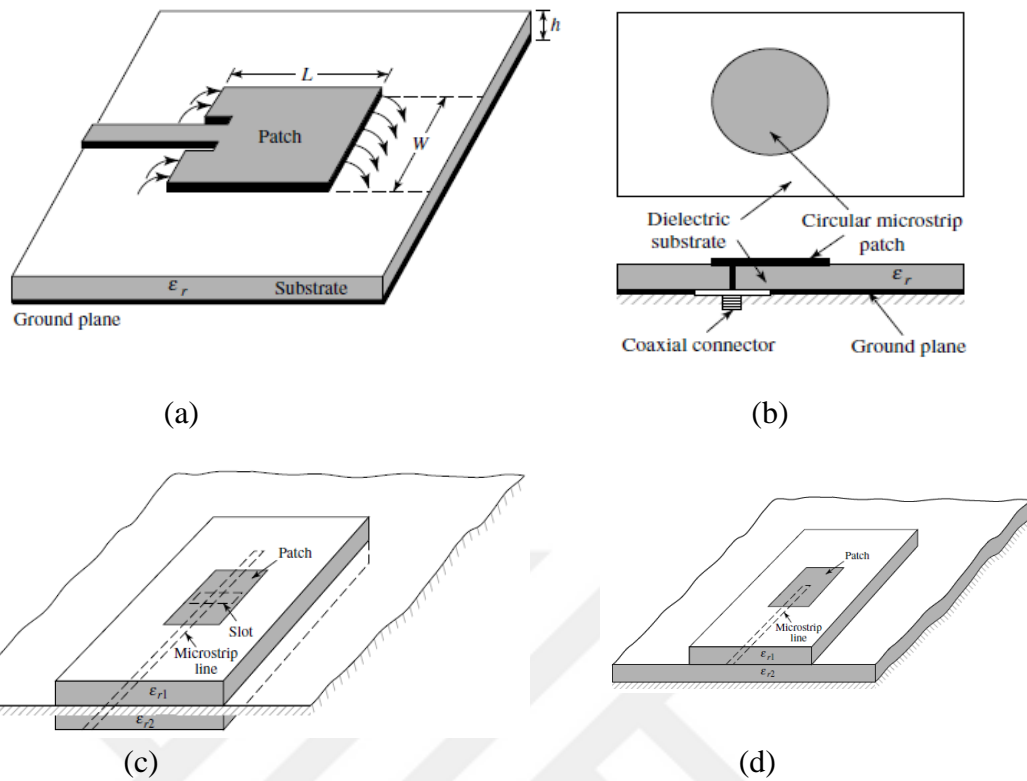


Figure 2.13 Types of feeding methods (a) microstrip line feed, (b) probe feed, (c) aperture-coupled feed, (d) proximity-coupled feed (Balanis, 2005)

2.5 Method of Analysis

Microstrip antennas can be analyzed with various methods. Transmission line model (TLM) and Cavity model are two of them. Although TLM can be applied for only rectangular or square geometries, cavity model can be applied for rectangular, square and more geometries. On the other hand, reliable results especially in upper frequencies are not given by TLM. However, the results obtained from cavity model are more reliable than TLM (Çakır, 2004).

Microstrip antenna is considered as a cavity bounded with perfect magnetic walls on the edges and perfect electric conductors on the lower and upper planes in cavity model (James & Hall, 1989).

Although TLM and cavity model are basic and useful methods, which make physical insight about the radiation mechanism of the antenna, they are approximate

and their certainties are less than full-wave analysis methods. Numerical solution of integral and/or differential equations are the basis of full-wave analysis methods (Balanis, 2005; Yildirim, 2010). Method of Moments (MoM), Finite Element Method (FEM), Finite Difference Time Domain (FDTD), Finite Integration Technique (FIT), Finite Volume Time Domain (FVTD) are some examples.

Accuracy of the full-wave techniques are potentially very high. The main idea of the all methods under the full-wave techniques is to discretize some unknown electromagnetic property, for instance, \vec{E} field for the FEM and FDTD method, the surface current for the MoM (For the latter, \vec{H} the field is also discretized). This procedure is termed as meshing (Davidson, 2005).

Techniques, which can be divided under the full-wave methods, can be categorized as partial differential equation (PDE) based or integral equation (IE) based. Because, Maxwell's equations can be written in either differential or integral form (Stutzman & Thiele, 2013). Figure 2.14 classifies the full wave methods.

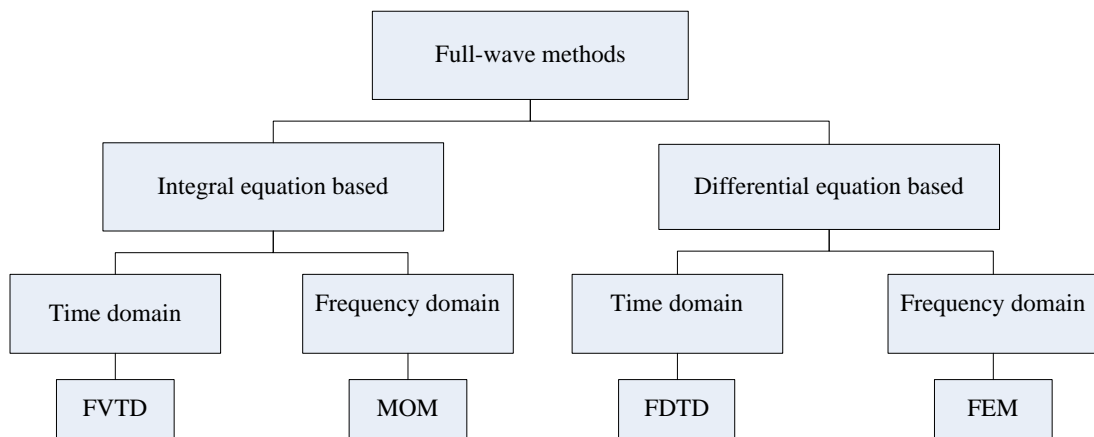


Figure 2.14 Classification of full wave methods

There are many electromagnetic simulator software in the market which use different numerical solving techniques. Table 2.2 divides electromagnetic simulation programs to their numerical solving techniques.

Table 2.2 Some of the electromagnetic simulation programs to their numerical solving techniques

FEM	MOM	FDTD
High Frequency Structural Simulator (HFSS)	Advanced Design System (ADS) Momentum	Computer Simulation Technology (CST)

CST MICROWAVE STUDIO and REMCON's XFDTD; the former actually uses the Finite Integration Technique, but this is very closely related to the FDTD (Davidson, 2005).

2.5.1 Finite Difference Time Domain (FDTD) Method and Difference between FDTD and Finite Integration Technique (FIT) Methods

According to Stutzman & Thiele, (2013) "The basis of the FDTD algorithm is the two Maxwell curl equations in derivative form in the time domain. These equations are expressed in linearized form by means of central finite differencing. Only nearest-neighbor interactions need be considered as the fields are advanced temporally in discrete time steps over spatial cells usually of rectangular shape as indicated in Figure 2.15 other cell shapes are possible, as well as two-dimensional and one-dimensional treatments."

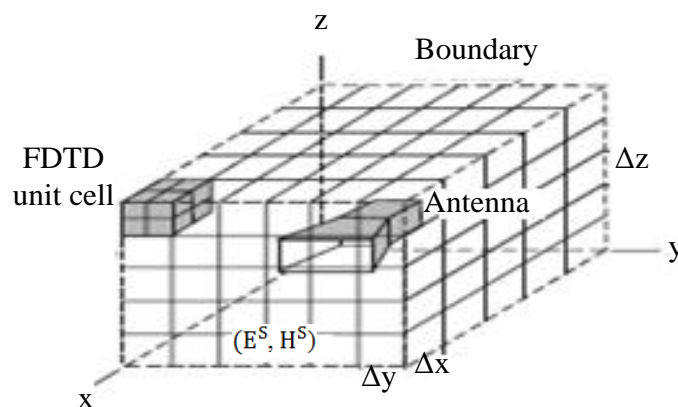


Figure 2.15 Embedding of an antenna structure of an antenna in an FDTD (Stutzman &Thiele, 2012)

This method employs all positional and time derivatives of the Maxwell's equation by using finite-difference approximations which is called Yee's algorithm. The original grid in the Yee algorithm is a Cartesian grid with structured cells, where electric field and magnetic components are placed in a staggered regulation (Rahimi, 2011).

Considering a uniform rectangular grid with spatial grid sizes Δx ; Δy ; Δz , the space point lattices are:

$$(x, y, z) = i\Delta x, j\Delta y, k\Delta z \quad (2.25)$$

where $i, j, k = 0, 1, 2, \dots$. For a time step size Δt , a time derivative of an arbitrary quantity $U(x, y, z, t) = U^n(i, j, k)$, where $t = n\Delta t$, can be discretized by central finite-difference equations as

$$\frac{\partial U(x,y,z,t)}{\partial t} = \frac{1}{\Delta t} \left[U^{n+\frac{1}{2}}(i, j, k) - U^{n-\frac{1}{2}}(i, j, k) \right] + O[(\Delta t)^2], \quad (2.26)$$

and the curl operator can be discretized as

$$\begin{aligned} \Delta_x \times U(x, y, z, t) &= \frac{1}{\Delta y} \left[U_z^n \left(i, j + \frac{1}{2}, k \right) - U_z^n \left(i, j - \frac{1}{2}, k \right) \right] - \\ &\frac{1}{\Delta z} \left[U_y^n \left(i, j, k + \frac{1}{2} \right) - U_y^n \left(i, j, k - \frac{1}{2} \right) \right] + O[(\Delta y)^2] + (\Delta z)^2]. \end{aligned} \quad (2.27)$$

According to (Kahnert, 2002; Taove & Hagness, 2000); "Maxwell's equations are then numerically solved through time-stepping of the set of equations. A plane wave propagates through the discretized spatial domain and field components are updated, at each discrete time step, using the previous time step field results. In order to obtain convergent solutions, the time step should satisfy the Courante-Friedrich-Levy (CFL) condition, where the time step is confined by a factor of the spatial mesh size."

$$\Delta t \leq \frac{1}{c} \sqrt{\frac{1}{\Delta x^2} + \frac{1}{\Delta y^2} + \frac{1}{\Delta z^2}} \quad (2.28)$$

where c is speed of light in free space (Kahnert, 2002; Taove & Hagness, 2000).

The time domain formulation of the FDTD method has some considerable properties. One of them, using wideband sources, the FDTD method can compute a wideband response in one run. However, the frequency domain methods must compute the system response for every frequency point separately (Taflove, 1998).

Davidson (2005), conclude the FDTD method as “It is the preferred method for wideband systems. Even in its standard Yee form, it is also a strong contender for any electromagnetic radiation or scattering problem for which quick answers are needed, great accuracy is not the primary concern, and quite large run-times and memory usage is acceptable.”

FDTD and FIT are similar methods for homogeneous media. However, the FIT transforms Maxwell's equations, in their integral form, to a linear system of equations. Interfaces between different medium are treated in a more correct manner by FIT method. Curved boundaries and complicated shapes are processed more flexible with more accuracy (Rahimi, 2011).

2.6 CST Microwave Studio

Computer Simulation Technology AG developed CST Studio Suite (CST). CST contains CST's tools, and the design and optimization of structures over wide range of frequencies are done by the help of these tools. CST includes a number of modules. CST Microwave Studio (CST MWS) is an appropriate module to simulate antennas (Chan, 2011).

For three dimensional EM simulation of high frequency problem CST MWS is a specialist tool (CST, 2014). The range of simulation methods in CST MWS give an

opportunity to the users to select the best technique for each application. For wideband or planar antennas, one of the option can be the transient solver. For electrically small antennas the frequency domain solver can be more convenient. Electrically large or wire antennas can efficiently simulate by using integral equation solver (CST, 2014). The antennas in this thesis are simulated by using transient solver of CST MWS.

In order to gain the best simulation results in CST, several settings should be configured such as mesh type, boundary conditions, frequency range and field monitors. Settings of mesh properties under the global properties is chosen default value. It is hexahedral type, 10 lines per wavelength and 10 cells per max model box edge. The boundary conditions are also set to the default value. The X_{\min} , X_{\max} , Y_{\min} , Y_{\max} , Z_{\min} and Z_{\max} boundaries are chosen “open (add space)”. The dimensions and frequency under the unit settings are defined in Millimeter and Gigahertz respectively. The Minimum frequency (F_{\min}) and Maximum frequency (F_{\max}) under the frequency range settings are chosen 0.75 GHz and 3 GHz respectively in the simulations.

2.7 Anechoic Chamber

Anechoic chamber is an alternative to outdoor measurements to obtain a controlled environment an all-weather conditions and security, and provide minimum electromagnetic interference. Measurements can be done inside a chamber by using this technique. RF absorbing material has provided the impulse for the development and generation of anechoic chambers (Balanis, 2005).

The rectangular and the tapered chambers are two common types of anechoic chamber designs, which are inspired by geometrical optics techniques with the purpose to decrease specular reflections (Balanis, 2005).

The purpose of designing the rectangular chamber is to simulate free-space conditions and creating maximum quiet area. The pattern and location of the source,

operation frequencies are considered in the design, and it supposes that the receiving antenna at the test point is isotropic. Usage of high quality RF absorbers minimizes reflected energy (Gillette & Wu, 1977; Balanis, 2005).

Balanis (2005), describes Tapered Anechoic Chambers by the help of Emerson & Sefton (1965), study as “take the form of a pyramidal horn. They begin with a tapered chamber which leads to a rectangular configuration at the test region. At the lower end of the frequency band at which the chamber is designed, the source is usually placed near the apex so that the reflections from the side walls, which contribute to the illuminating fields in the region of the test antenna, occur near the source antenna.”

In this thesis a rectangular type small-size Radio Frequency Anechoic Chamber, which is located in Dokuz Eylül University Antenna and Microwave Technique Laboratory as shown in Figure 2.16 is used to measure some of the parameters of the antennas.

The small-size RF anechoic chamber in Figure 2.16 has the dimensions of 1 m x 1 m x 1.5 m. The outer conductor of the chamber is stainless steel. The chamber is coated with RF absorbers inside (Seçkin Uğurlu, Özgönül, Özkurt & Seçmen, 2015).



(a)



(b)

Figure 2.16 RF anechoic chamber (a) inner view, (b) closed view

CHAPTER THREE

THE DESIGN OF THE ANTENNAS AND RESULTS

In this chapter, the specifications and methodology to design the wide-band antennas as well as measurement process are demonstrated. Planar monopole antennas and log periodic dipole array antennas which are the types of studied antennas in the thesis are explained briefly. The simulation and measurement results of the antennas are presented by graphs and figures.

3.1 Specifications of the Antennas and Methodology

Specifications of the antennas can be divided into four important parameters:

- **Operating Frequency:** Antennas have wide operating frequency range between 0.75 GHz to 3 GHz and are convenient to GPS (1227.60 MHz, 1575.42 MHz), GSM (900MHz), 3G (2100 MHz), Wi-Fi (2400 MHz), and LTE (2600 MHz) wireless systems. The return loss should be at least 10 dB for the given range.
- **Farfield condition:** Lengths of the antennas are determined to satisfy most commonly used farfield condition which is given in (2.16) for used anechoic chamber almost all operating frequency band.
- **Cheap:** FR4 dielectric substrate with dielectric constant (ϵ_r) = 4.4 and 0.025 lost tangent is selected. This substrate has been selected since being inexpensive.
- **Small volume:** Standard 1.6 mm height (h) FR4 substrate is selected. The antenna has the maximum sizes in the thesis have 174 mm \times 147 mm \times 1.6 mm dimensions.

Firstly, theoretical study and literature search are done to design wide-band antennas. Printed planar monopole antenna and printed log periodic dipole array antenna are decided to design. Then, literature search is done for these types of antennas. Printed planar monopole and a printed log periodic dipole array antennas are designed based on the literature. Design and simulation of the antennas are carried out by using CST Microwave Studio. The antennas (which have desired simulation results) are manufactured. The produced antennas are measured. Then, simulation and measurement results are compared. Antennas which have good agreement are taken as successful. Others which do not satisfy the given specifications are considered as unsuccessful and are modified to give better results. Figure 3.1 shows flow chart of methodology starting from design and simulation step. Also, a Koch Fractal log periodic dipole array antenna is designed, simulated and manufactured based on the literature.

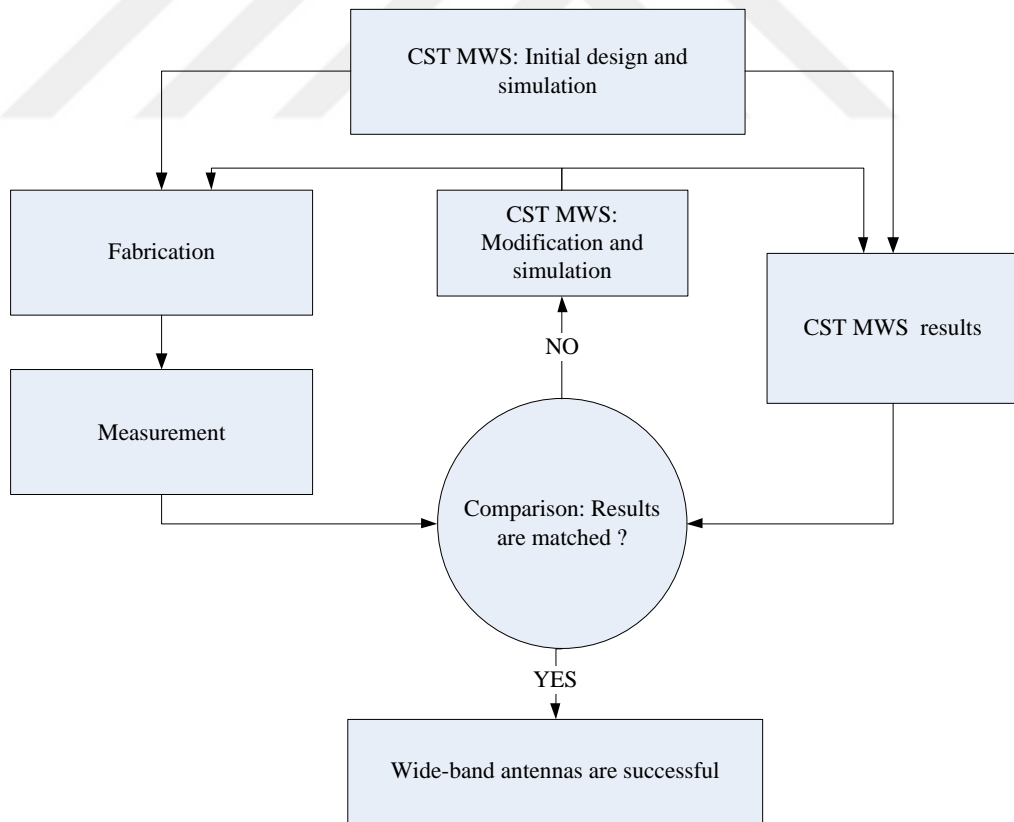


Figure 3.1 Flow chart for design methodology

3.2 Measurement Process

The presented antennas are fabricated on both side of the low-cost FR4 dielectric substrate by using printed circuit techniques with a height of $h = 1.6$ mm, dielectric constant of 4.4 and loss tangent of 0.025. Then, some parameters are measured to define the performance of the antenna. In this thesis; S_{11} , antenna radiation pattern and gain parameters are measured. Measurement results are compared with simulation results.

Radio Frequency (RF) network analyzer is one of the most commonly used test equipment which classifies frequencies in terms of character and response. RF network analyzers are usually associated with microwave frequencies. Scalar network analyzer (SNA), vector network analyzer (VNA), and large signal network analyzer (LSNA) are some examples of RF network analyzers (Poole, n.d.).

VNA is a device which is used to characterize the performance of RF and microwave devices in terms of network scattering parameters or S parameters. The data gathered by VNA lead to optimize the design of RF circuit to provide the best performance (Poole, n.d.).

Return Loss antenna parameter of manufactured antennas are measured by Anritsu MS4642A Vector Network Analyzer (VNA), which is located in Dokuz Eylül University Antenna and Microwave Technique Laboratory and photographed in Figure 3.2.

In order to obtain the best results of VNA measurements, proper calibration process which use vector error correction technique should be done. This is because calibration prevents systematic errors and reduce measurement uncertainty. While performing calibration, good quality equipment should be used. Finally, the calibration should be checked generally measuring scattering parameters of short, open and load (generally 50 or 75 ohm).



Figure 3.2 Anritsu MS4642A VNA (Anritsu, 2015)

The radiation pattern and gain parameters of the manufactured antennas are measured to understand gain and radiation characteristics of the antennas.

Antenna patterns can be displayed in various types. One way is the plot in polar type. Moreover, the scale can be linear or logarithmic (decibel). Some combinations of plot type and scale type can be used such as polar-linear, polar-log. In the thesis, patterns are given polar-log type (Stutzman & Thiele, 2013).

To obtain radiation properties of an antenna, it is necessary to measure all angles (θ , ϕ). It needs some laboratory equipment measuring and recording data. In practice, radiation pattern is measured in E-plane and H-plane.

The measurement set is prepared to define the radiation pattern of the test antenna. This set basically consists of four main parts. They are transmitting, positioning, receiving and display. RF source and transmitting antenna are elements of transmitting part. This antenna is the commercial log periodic dipole array. Rotational positioner is a component of positioning part. In this part, the test antenna mounted on positioner and is rotated about the azimuth. In receiving part, network analyzer and test antenna are used. Two dimensional polar patterns include E-plane and H-plane patterns which are plotted via the software used for display part.

According to the Balanis (2005), there are two basic methods to measure gain of an antenna, which are absolute-gain and gain-transfer methods. In this thesis gain-transfer method is used for the gain measurement. This method utilizes a gain standard (with a known gain) to determine absolute gain. Furthermore, gain transfer method is based on Friis Transmission Formula.

The Friis Transmission Equation relates the power received to the power transmitted between two antennas separated by a distance $R > 2D^2/\lambda$, where D is the largest dimension of either antenna (Balanis, 2005). For reflection and polarization-matched antennas, Friis Transmission Equation can be written as

$$P_r = P_t \frac{G_t G_r \lambda^2}{(4\pi R)^2} \quad (3.1)$$

where; P_r is received power (Watt), P_t is input power (Watt), R is the separation between antennas (m), G_t is gain of the transmit antenna, G_r is gain of the received antenna.

Free-space loss factor is $(\lambda/4\pi R)^2$, and it considers the losses because of the spherical spreading of the energy by the antenna (Balanis, 2005).

By the help of Friis Transmission Equation, formula of gain in dB with transfer method is written according to the Balanis (2005), as

$$(G_t)(\text{dB}) = (G_s)(\text{dB}) + 10 \log_{10} \left(\frac{P_t}{P_s} \right) \quad (3.2)$$

where; $(G_t)(\text{dB})$ and $(G_s)(\text{dB})$ are the gains (in dB) of the test and standard gain antennas respectively.

3.3 The Realization of the Printed Planar Monopole Antennas

The last few years wireless systems developed rapidly. For this purpose, numerous antenna designs including wideband characteristics have been presented with different types (Yadaw & Pahwa, 2014; Ávila-Navarro & Reig, 2012). Wideband antennas have been interesting subject due to being an important component for many civil and military applications such as radar and communication systems. Monopole antennas with planar radiators have broad bandwidth, simple structure and can be easily printed on a dielectric substrate which called printed planar monopole antenna (Liang, Chiau, Chen & Parini, 2005). Due to these properties planar monopole antennas is an important candidate for these applications.

In 1968, Meinke and Gundlach introduced monopole antennas with planar radiating elements firstly. They defined it as a variant of the conical and cylindrical monopole. In 1976, Dubost and Zisler define in more detail. The impedance and radiation characteristics of this antenna are studied by them. Various geometries for the planar element have been presented. They have mostly based on the circular and square shapes (Evans & Ammann, 2004; Meinke & Gundlach, 1968; Dubost & Zisler, 1976; Agrawall, Kumar, and Ray, 1998; Ammann, 1999). Printed planar monopole antenna basically consists of three main parts as shown in Figure 3.3. These are ground, feeding line and patch.

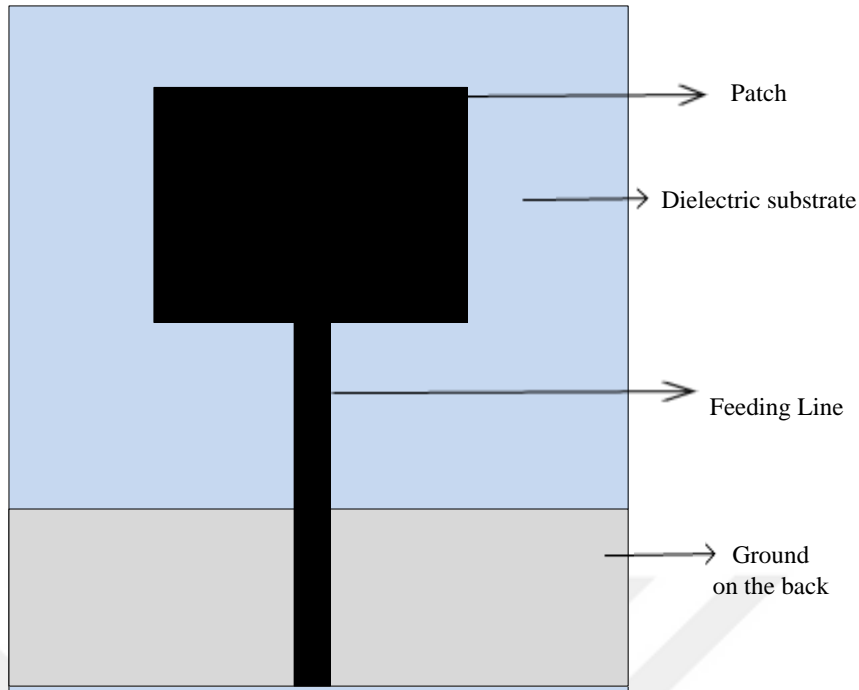


Figure 3.3 Basic shape of printed planar monopole antenna

The form of printed monopole antenna is similar with microstrip patch antenna. However, they have different ground plane structure and printed monopoles have larger impedance bandwidths than microstrip patch antennas. However, designing a printed planar monopole is a complex process such that here is no exact formulas or mathematical expressions. Under this circumstance, the design of a planar monopole is based on the performance of the design parameters such as shape of the radiating patch, width and length of the ground plane. Parametric studies provide us some rough ideas to figure the role of investigated parameter on the performance of the antenna (Bozdağ, 2014; Moradikordalivand et al., 2014).

In this part of the chapter, printed planar monopole antennas containing of two different types have been simulated, fabricated and measured for the desired operating frequency range. Microstrip feed line is used. However, there are many different feeding methods which are mentioned in chapter two, microstrip feeding can be easily designed and fabricated.

In the first printed planar monopole antenna design, printed disc monopole fed by 50Ω microstrip line is used and modified which is proposed by Liang et al. (2005).

Antenna parameters such as length and width of the either substrate or ground plane and radius of the circular disc are optimized by using the parametric sweep tool of the CST Microwave Studio for desired operating frequency range with nearly omnidirectional radiation pattern.

The printed circular disc planar monopole antenna is illustrated on Figure 3.4.

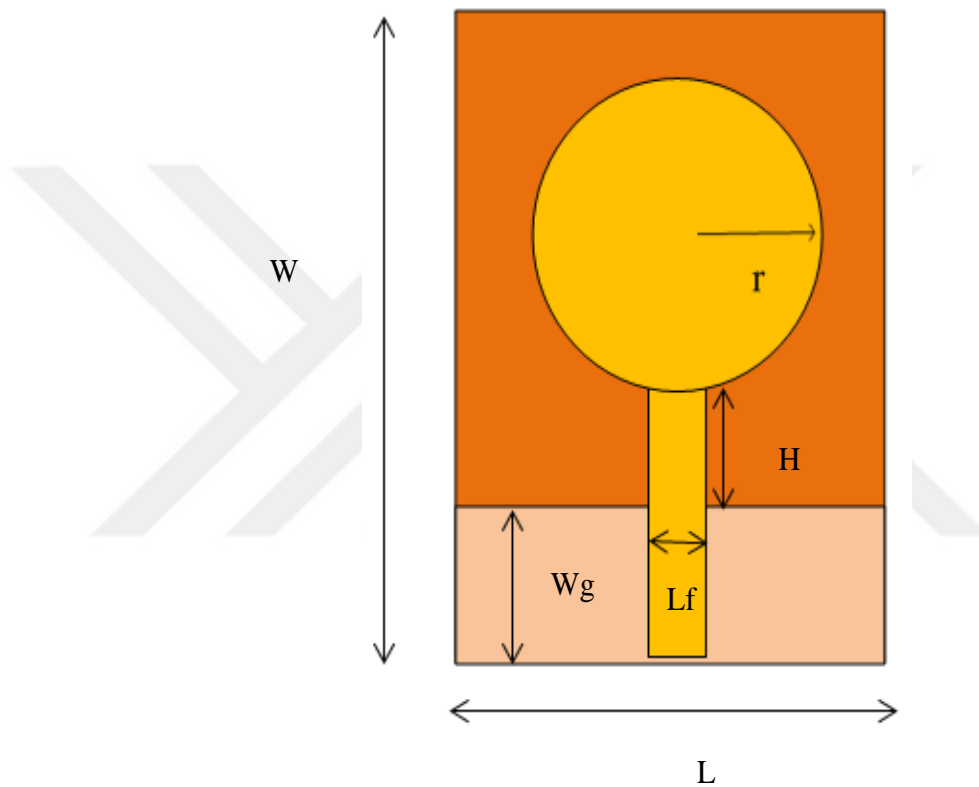


Figure 3.4 Geometry of the printed circular disc planar monopole antenna

Here, a printed circular disc monopole antenna has a radius of r , W is length and L is width of the FR4 substrate, L_f is width of the feed line. On the opposite site of the substrate, W_g denote length of the ground plane and H is the height of the distance between the circular disc and the ground plane. After parametric sweep, obtained optimal design parameters for desired frequency range is shown in Table 3.1.

Table 3.1 Optimal design parameters for the printed circular disc planar monopole antenna

r	W	L	Lf	Wg	H
72 mm	157 mm	116 mm	3 mm	42mm	0.3 mm

The printed circular disc monopole with optimal parameters is realized on the dielectric substrate whose simulated and manufactured views are shown in Figure 3.5 and Figure 3.6 respectively.

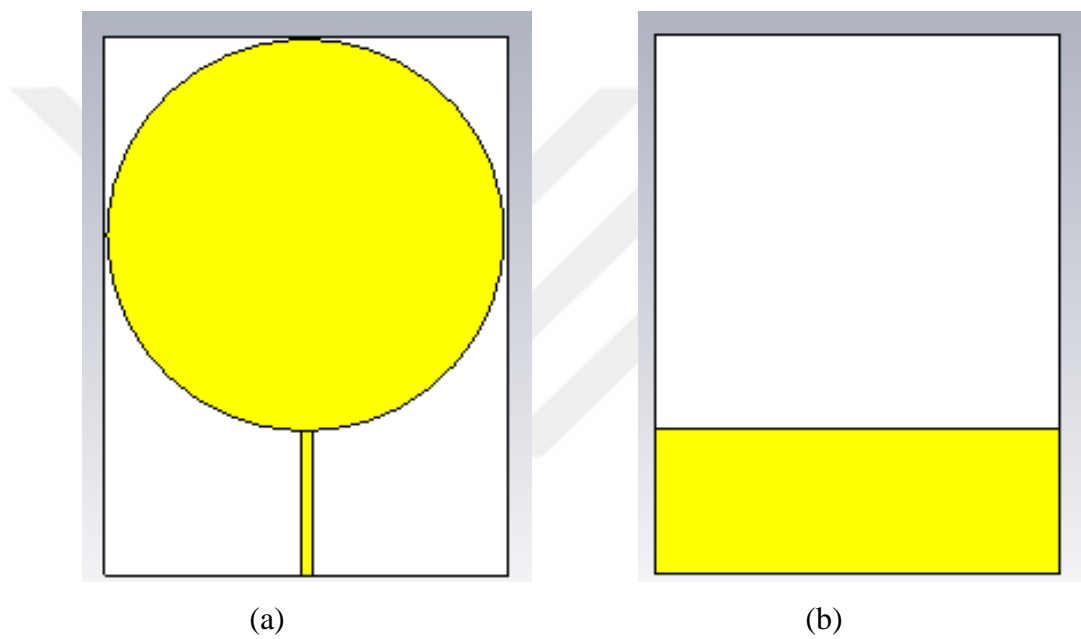


Figure 3.5 The printed circular disc planar monopole antenna. Modeled in CST Microwave Studio (a) top view, (b) bottom view

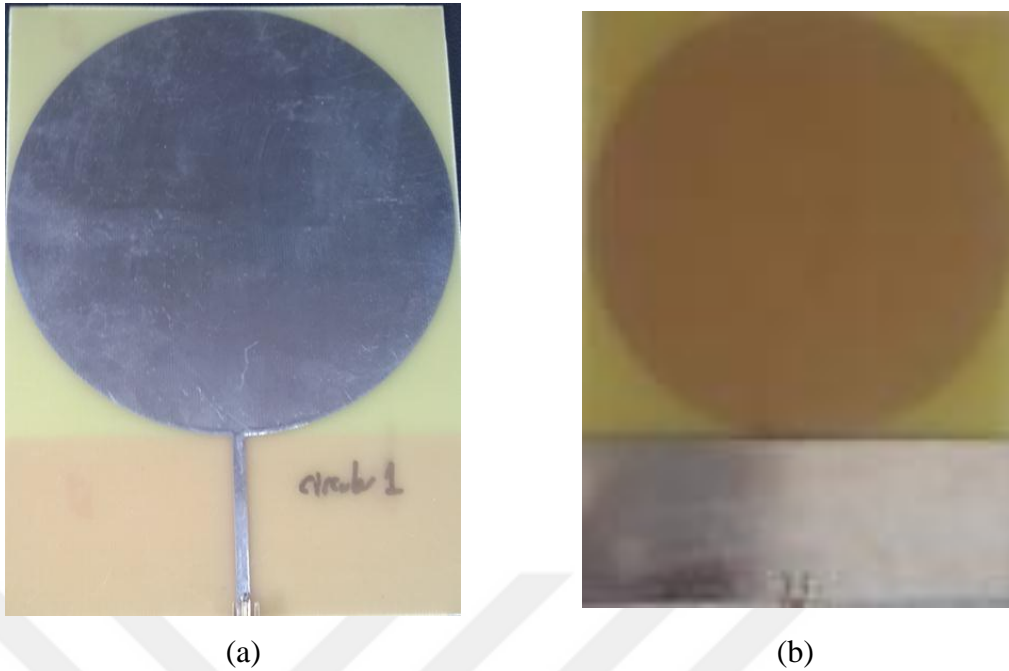


Figure 3.6 Realization of the printed circular disc planar monopole antenna (a) top view, (b) bottom view

The measurement S_{11} is compared with simulation result. There is a good agreement between them. Figure 3.7 shows comparison of measured and simulated S_{11} for the antenna.



Figure 3.7 Comparison of measured and simulated S_{11} for the printed circular disc planar monopole antenna (--- measurement, — simulation)

Other performance parameters of the antenna are investigated. Figure 3.8 and Figure 3.9 give normalized E-plane and H-plane radiation patterns respectively. Also, in Table 3.2 calculated and simulated broadside gains are given.

Table 3.2 Calculated and simulated broadside gains for different frequencies for printed circular disc planar monopole antenna

Frequency	Calculated Gain	Simulated Gain
1 GHz	2.2 dB	2.4 dB
1.5 GHz	1 dB	1.7 dB
2 GHz	-1.5 dB	-2.9 dB
2.5 GHz	-3.5 dB	-6 dB
3 GHz	-12.5 dB	-14 dB

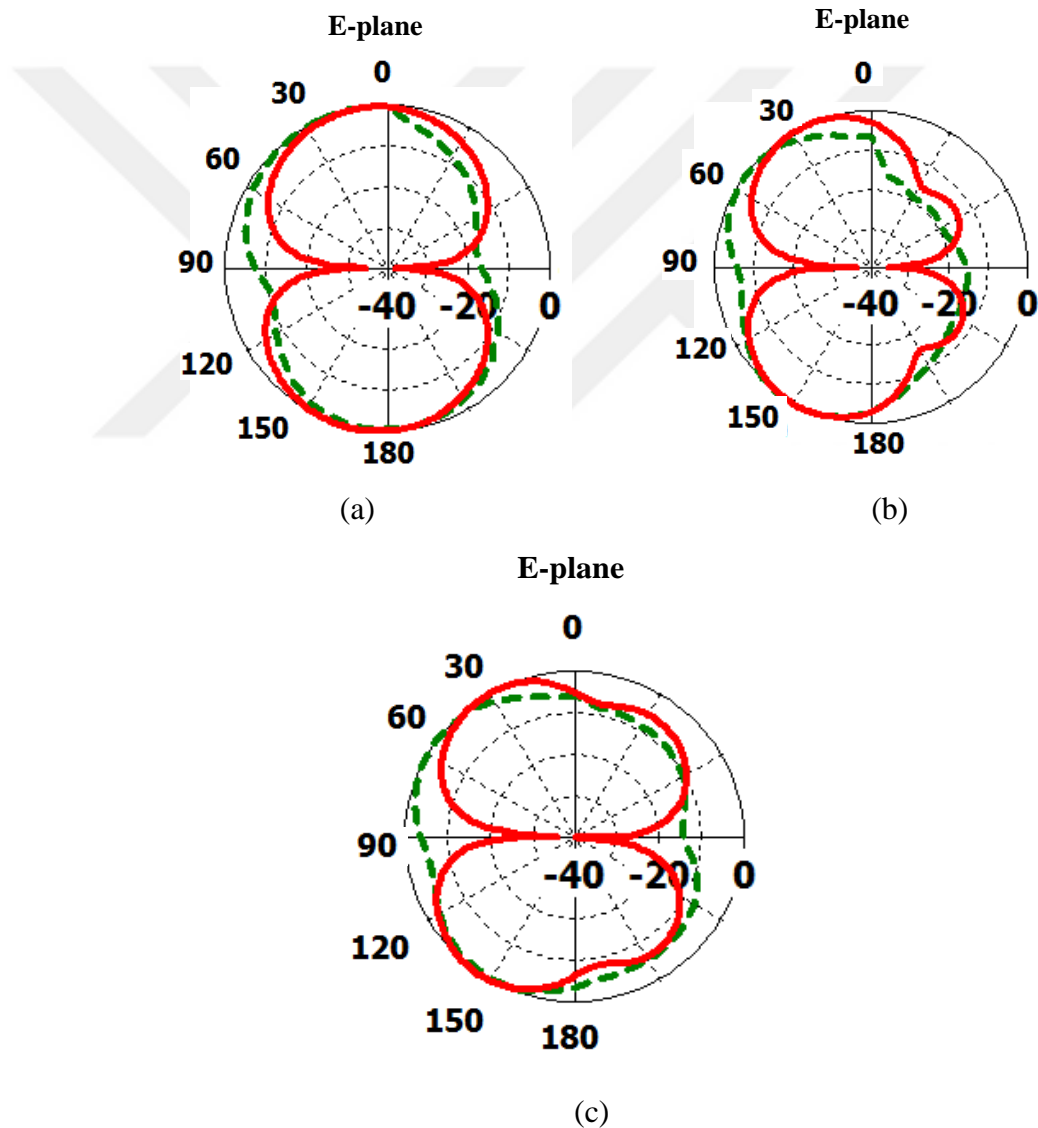
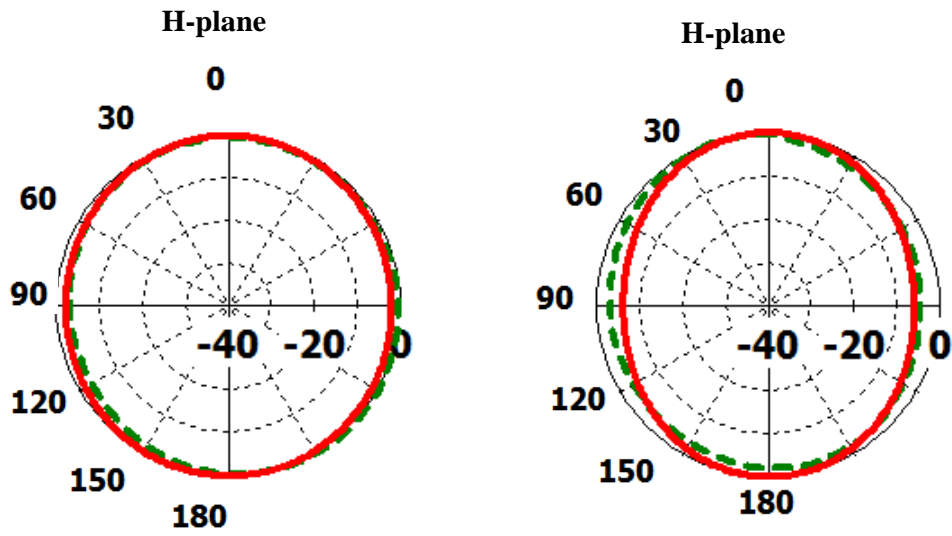
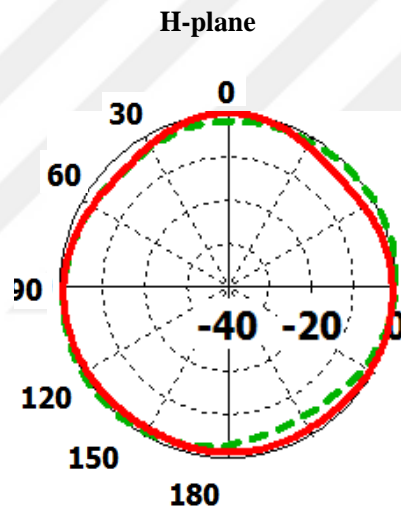


Figure 3.8 Measured and simulated E-plane polar radiation patterns of the circular disc printed planar monopole antenna (--- measurement, — simulation) at (a) 1 GHz, (b) 1.5 GHz, (c) 2 GHz



(a)

(b)



(c)

Figure 3.9 Measured and simulated H-plane polar radiation patterns of circular disc printed planar monopole antenna (--- measurement, — simulation) at (a) 1 GHz, (b) 1.5 GHz, (c) 2 GHz

Good agreement between calculated and simulated broadside gains are observed for circular disc printed planar monopole antenna. However, maximum 2.5 dB deviation is observed in the given frequencies in the Table 3.2. On the other hand, measured normalized H-plane and E-plane radiation patterns are matched well with simulation results.

In the second printed planar monopole antenna, broadband modified rectangular microstrip-fed monopole antenna using stepped cut at four corners (SCFC) method which is proposed by Moradikordalivand et al., (2014) is used and T-shape slot is employed to the ground surface (J.J. Jiao, Zhao, Zhang, Yuan & Y. C. Jiao, 2007; Chaiteang, et al., 2014) to increase bandwidth at desired frequency range.

To achieve wide frequency bandwidth, in the stepped cut at four corners (SCFC) method can be applied to the rectangular patch. At the beginning of the process, the lower and the upper frequencies (F_L and F_H respectively) of working frequency range must be determined. Second step is to define dimensions of the patches by using transmission line equations. Then, in order to operate full frequency band between upper and lower frequencies, new patches are created (related to F_1 to F_{n-1}). Finally, step cutting positions are defined by illustrating the orthogonal lines from the corners of the inner patches to the border lines of outer patch. Structure position of the patches is shown in Figure 3.10. Designed patch numbers in the F_L patch are indicated by n . Graph plane with $1/n$ spacing is formed at the corners (Moradikordalivand et al., 2014).

The length (W_L) and the width (L_L) of the rectangular patch can be calculated by the help of transmission line model calculations for rectangular patch (Balanis, 2005, Moradikordalivand et al., 2014). In the thesis the length and the width of the rectangular patch are 126 mm and 103 mm respectively.

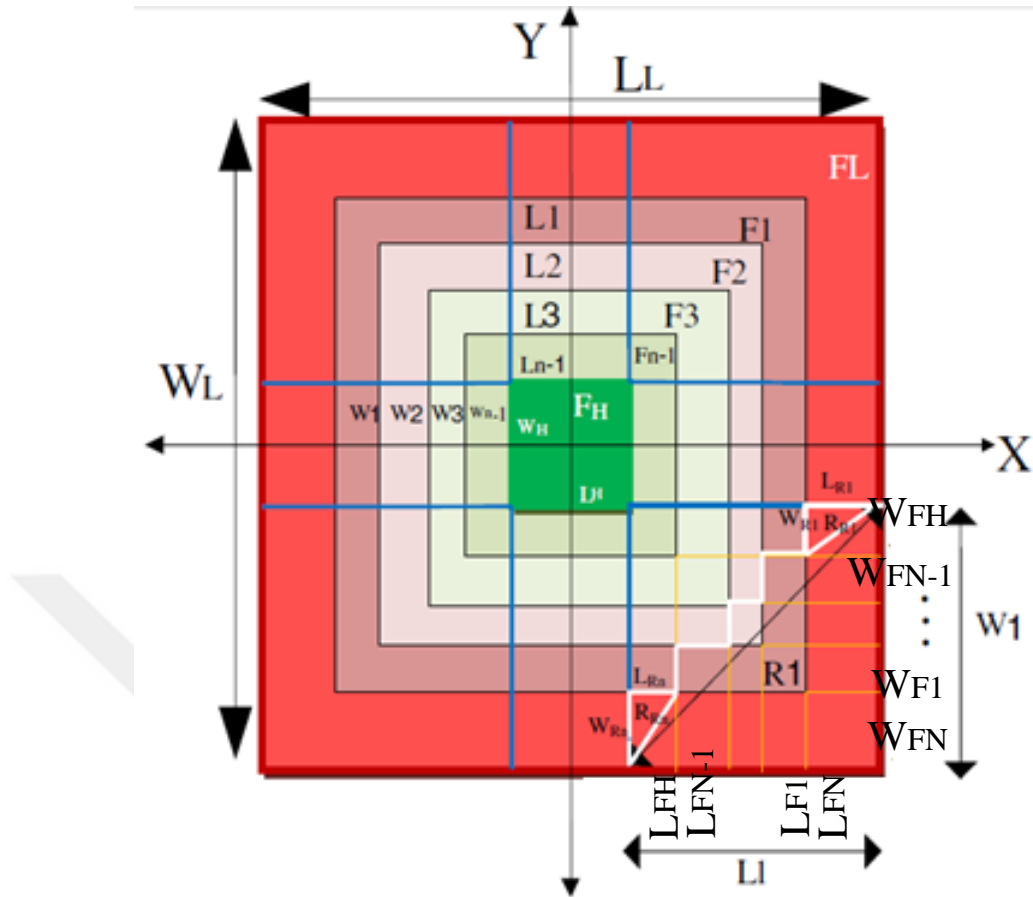


Figure 3.10 Configuration position of the patches in the SCFC method (Moradikordalivand et al., 2014)

Some parameters need to be calculated for optimal design. Moradikordalivand et al. (2014), gives formulas for calculating these parameters.

Next, equations are used to calculate the sizes of the steps at the corners as

$$W_1 = \frac{W_L - W_H}{2} \quad (3.3)$$

$$L_1 = \frac{L_L - L_H}{2} \quad (3.4)$$

where the width and the length of FL patch are indicated by W_L and L_L respectively. Also, W_H and L_H indicate the width and the length of FH patch respectively.

where the step dimensions are same, and:

$$W_R = \frac{W1}{n} \quad (3.5)$$

$$L_R = \frac{W1}{n} \quad (3.6)$$

$$R_1 = n \times \sqrt{L_R^2 + W_R^2} \quad (3.7)$$

where the number of steps is represented by n, R_1 is stepped path, W_R is width of each step and L_R is length of each step. Otherwise:

$$\{W_{Rn}(n)\} = \begin{cases} W1 & n = 1 \\ W_{Fn-1} - W_{Fn} & 2 \leq n < \infty \end{cases} \quad (3.8)$$

where $W_{FH} = W_{Fn}$, $W_{FL} = W_{F0}$, W_{F1} to W_{Fn-1} are patches width position on the y-axis and $W_{R1} - W_{Rn}$ are step width.

$$\{L_{Rn}(n)\} = \begin{cases} L1 & n = 1 \\ L_{Fn-1} - L_{Fn} & 2 \leq n < \infty \end{cases} \quad (3.9)$$

where $L_{FH} = L_{Fn}$ and $L_{FL} = L_{F0}$

$$R_{Rn} = \sqrt{L_{Rn}^2 + W_{Rn}^2} \quad (3.10)$$

$$R_1 = \sum_{n=1}^{n=n} R_{Rn} = \sqrt{L_{R1}^2 + W_{R1}^2} + \sqrt{L_{R2}^2 + W_{R2}^2} \dots + \sqrt{L_{Rn}^2 + W_{Rn}^2} \quad (3.11)$$

$$= \sum_{n=1}^{n=n} \sqrt{L_{Rn}^2 + W_{Rn}^2}$$

where L_{F1} to L_{Fn-1} are patches length position on the x -axis and $L_{R1} - L_{Rn}$ are steps length (Moradikordalivand et al., 2014).

The geometry of the broadband modified rectangular monopole and simulated view of the antenna are illustrated in Figure 3.11 with top and forward views.

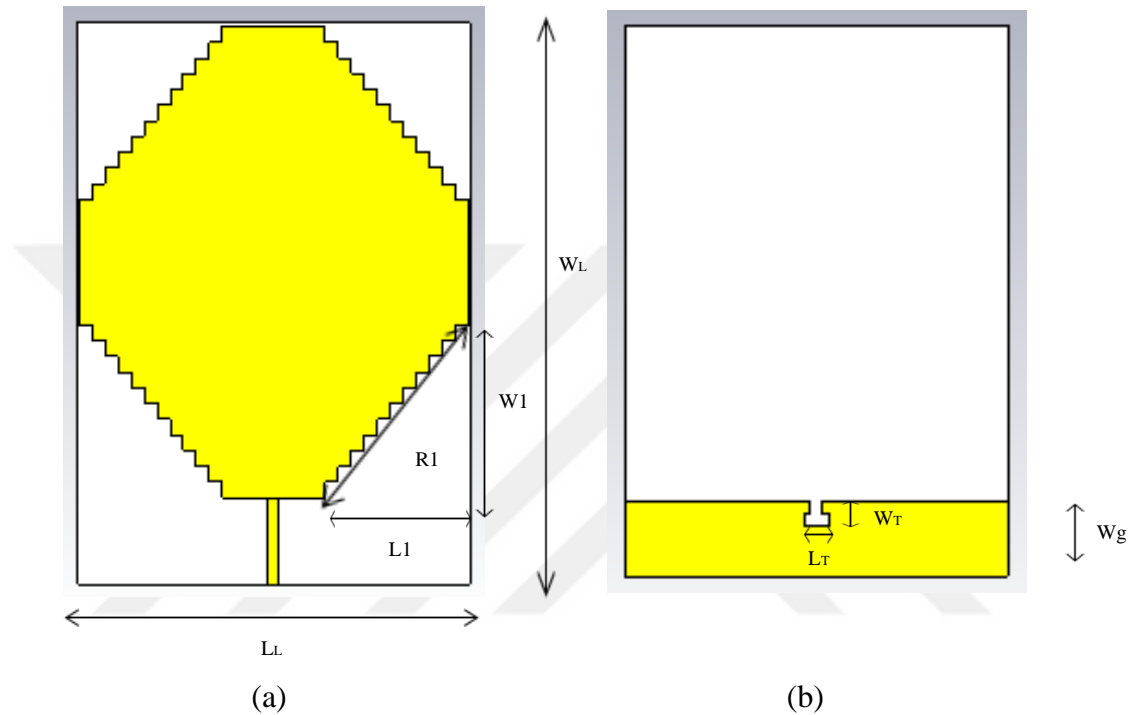


Figure 3.11 Geometry of the broadband modified rectangular planar monopole antenna. Modeled in CST Microwave Studio (a) top view, (b) forward view

Furthermore, the manufactured views are shown in Figure 3.12, and design parameters are given in Table 3.3.



(a)



(b)

Figure 3.12 Realization of the broadband modified rectangular planar monopole antenna (a) top view, (b) forward view

Table 3.3 Design parameters for broadband modified rectangular planar monopole antenna

LL	WL	L1	W1	R1	Wg	LT	WT
104 mm	150 mm	38 mm	46 mm	59.6 mm	20.3 mm	6.6 mm	6.6 mm

Simulation and measurement S_{11} , normalized E-plane and H-plane radiation patterns, broadside gains of the antenna are given in Figure 3.13, Figure 3.14, Figure 3.15, and Table 3.4 respectively.

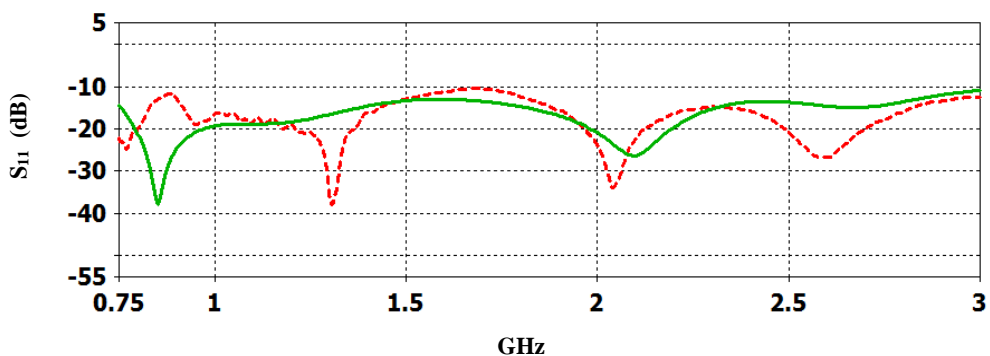


Figure 3.13 Simulation and measurement S_{11} of the broadband modified rectangular monopole antenna (--- measurement, — simulation)

Table 3.4 Calculated and simulated broadside gains for different frequencies for broadband modified rectangular planar monopole antenna

Frequency	Calculated Gain	Simulated Gain
1 GHz	3 dB	2.5 dB
1.5 GHz	-0.5 dB	-0.6 dB
2 GHz	-3.5 dB	-4.8 dB
2.5 GHz	-15 dB	-12 dB
3 GHz	-11 dB	-13 dB

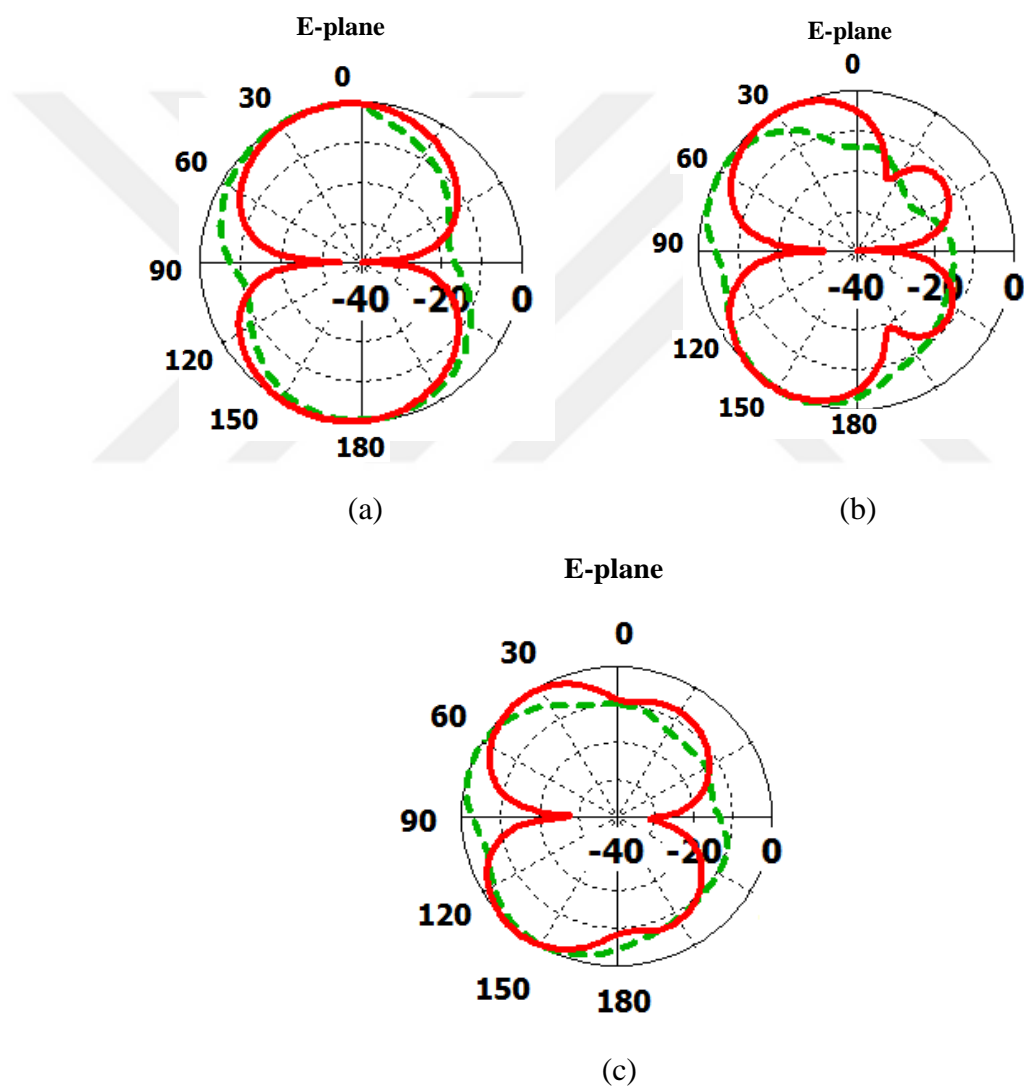


Figure 3.14 Measured and simulated E-plane polar radiation patterns of modified rectangular printed planar monopole (--- measurement, — simulation) at (a) 1 GHz, (b) 1.5 GHz, (c) 2 GHz

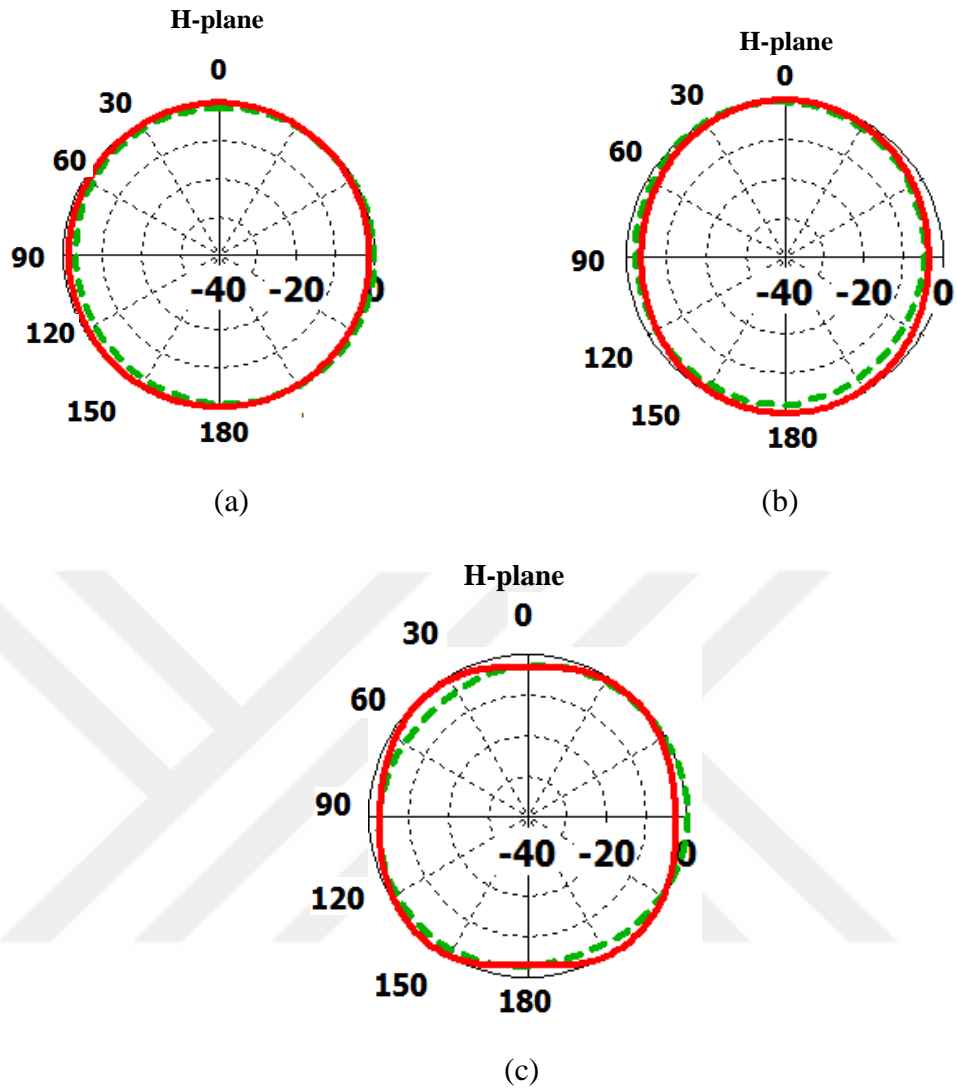


Figure 3.15 Measured and simulated H-plane polar radiation patterns of modified rectangular printed planar monopole (--- measurement, — simulation) at (a) 1 GHz, (b) 1.5 GHz, (c) 2 GHz

Good agreement between measured and simulated S_{11} is observed for modified rectangular printed planar monopole antenna, and there is almost a good agreement between calculated and simulated broadside gains with maximum 3 dB deviations in the given frequencies in the Table 3.4. On the other hand, good agreement between measured and simulated normalized H-plane and E-plane radiation patterns are observed.

3.4 Log Periodic Dipole Array Antenna

Log periodic antennas provide wide operation frequency bandwidth with acceptable gain. For these agreeable characteristics, log periodic antennas are used in many applications aiming to compact fabrication and nominal manufacturing cost. In general, log periodic antennas are used as either transmitting or receiving antennas for broadband applications. By tuning the relative dimensions of the longest and shortest elements of the array, the frequency bandwidth can be adjusted (Casula, Maxia, Mazzarella & Montisci, 2013; Balanis, 2005).

Figure 3.16 shows a well-known log-periodic structure. This structure introduced by DuHumell & Isbell (1957), and studied by Carrel (1961). Side-by-side linear dipoles forming a coplanar array occurs the structure. These antennas provide almost constant antenna performance parameters such as input impedance, return loss, radiation pattern over broad frequency range. On the other hand, log-periodic antenna can be designed easily. Parameters of the log periodic array such as lengths (l_n 's), spacings (R_n 's), diameters (d_n 's) of the log-periodic array changes logarithmically as described by the inverse of the geometric ratio tau (τ) (Balanis, 2005) which is given by equation (3.12).

$$\frac{1}{\tau} = \frac{l_2}{l_1} = \frac{l_{n+1}}{l_n} = \frac{R_2}{R_1} = \frac{R_{n+1}}{R_n} = \frac{d_2}{d_1} = \frac{d_{n+1}}{d_n} \quad (3.12)$$

Spacing factor (σ), which describes the log-periodic performance, is an another parameter related with a log periodic dipole array and defined by equation (3.13).

Moreover, straight lines to the dipole ends meet form degree of 2α . Generally, to design log-periodic dipole array antenna, α and τ selected as $10^\circ \leq \alpha \leq 45^\circ$ and $0.95 \geq \tau \geq 0.7$. There is an inverse relation between the values of α and τ . If α increases, τ decrease, and vice versa. To make a more compact design, higher values of α or lower values of τ is chosen, which needs smaller number of elements separated by longer distance (Balanis, 2005).

$$\sigma = \frac{R_{n+1} - R_n}{2l_{n+1}} \quad (3.13)$$

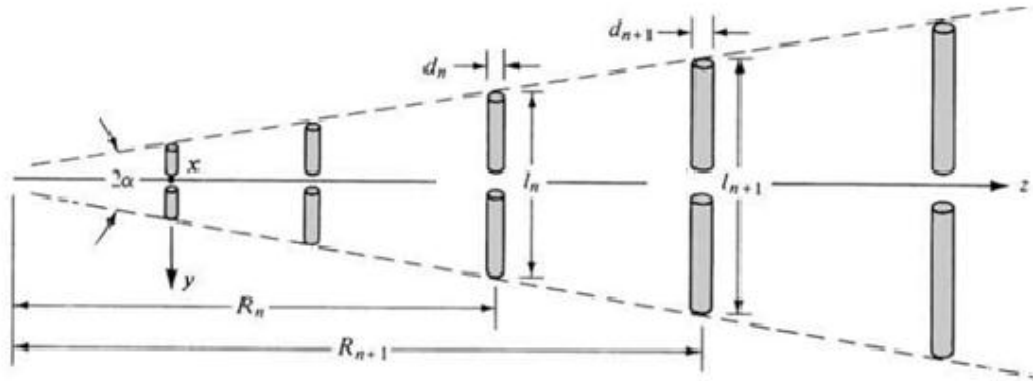


Figure 3.16 Log periodic dipole array (Balanis, 2005)

According to Balanis (2005), “all the elements of the log-periodic array are connected to the feed line and directly energized by the feed line. There are two basic methods, as shown in Figure 3.17 which could be used to connect and feed the elements of a log-periodic dipole array. In both cases, the antenna is fed at the small end of the structure. The currents in the elements of Figure 3.17 (a) have the same phase relationship as the terminal phases. If the elements are closely spaced in addition, the phase progression of the currents is to the right. This produces an end-fire beam in the direction of the longer elements and interference effects to the pattern result. It was recognized by mechanically crisscrossing or transposing the feed between adjacent elements, as shown in Figure 3.17 (b), a 180° phase is added to the terminal of each element. Since the phase between the adjacent closely spaced short elements is almost in opposition, very little energy is radiated by them and their interference effects are negligible. However, at the same time, the longer and larger spaced elements radiate.”

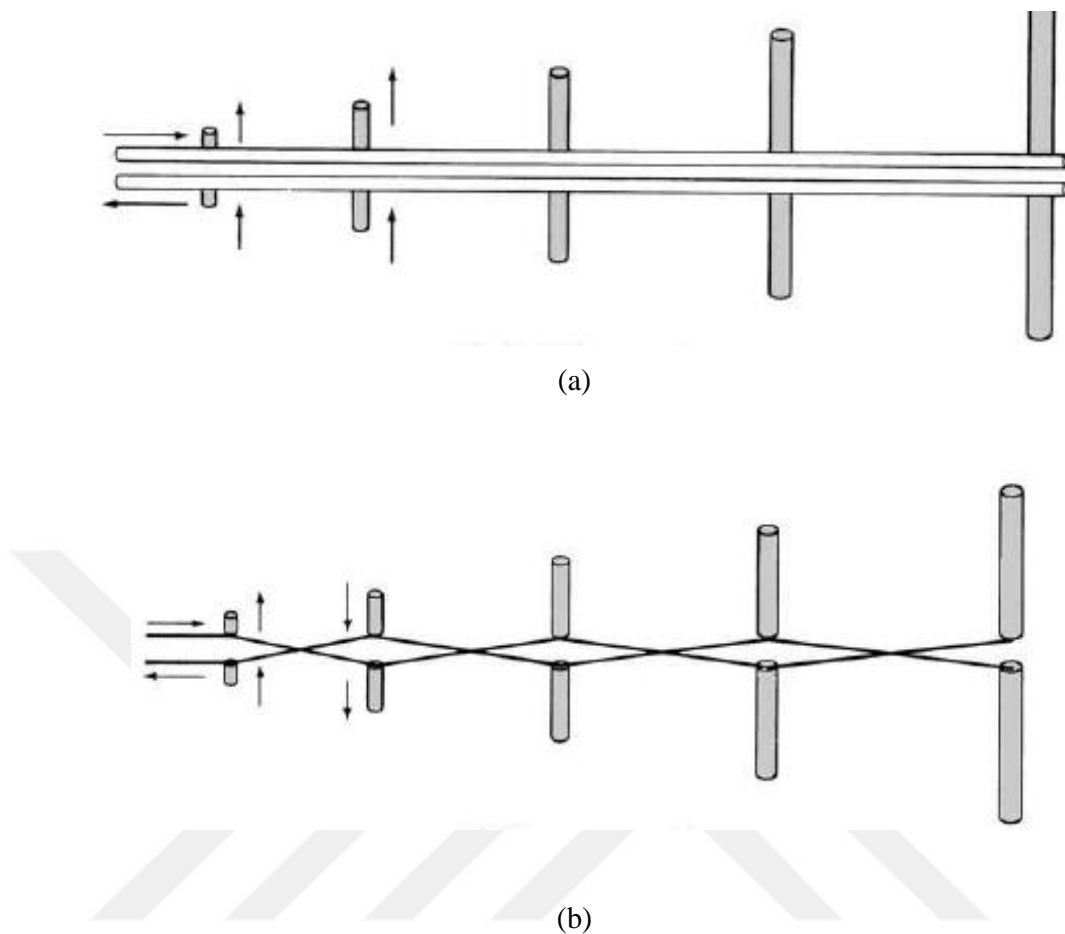


Figure 3.17 Log periodic array associated connections. (a) straight line, (b) crisscross (Balanis, 2005)

Moreover, Balanis (2005), gives that “If the geometrical pattern of the log-periodic array, as defined by (3.12), is to be maintained to achieve a truly log-periodic configuration, an infinite structure would result. However, to be useful as a practical broadband radiator, the structure is truncated at both ends. This limits the frequency of operation to a given bandwidth. The cutoff frequencies of the truncated structure can be determined by the electrical lengths of the longest and shortest elements of the structure. The lower cutoff frequency occurs approximately when the longest element is $\lambda/2$; however, the high cutoff frequency occurs when the shortest element is nearly $\lambda/2$ only when the active region is very narrow. Usually it extends beyond that element. The active region of the log-periodic dipole array is near the elements whose lengths are nearly or slightly smaller than $\lambda/2$. The role of active elements is passed from the longer to the shorter elements as the frequency increases.

Also the energy from the shorter active elements traveling toward the longer inactive elements decreases very rapidly so that a negligible amount is reflected from the truncated end.”

Due to having lower manufacturing cost and thinner profile, Printed Log Periodic Dipole Array Antennas (PLPDA) are more appropriate option than standard Log Periodic Dipole Array Antennas (LPDA), for many applications such as wideband systems and radar applications. Furthermore, LPDA and PLPDA are based on same conceptive idea (Bozdağ, 2014).

Practical design procedure proposed by Carrel (1961), is used with some modifications firstly. Then, some of the design parameters of the printed antennas are calculated.

The common configuration of a log-periodic array is given in terms of design parameters τ , α and σ related by

$$\alpha = \tan^{-1}\left[\frac{1 - \tau}{4\sigma}\right] \quad (3.14)$$

If two of them are defined, the other parameter can be found. Maximum directivity (in dB) can be estimated for a certain τ , utilizing optimal σ through the curves is given in Figure 3.18 (Balanis, 2005; Carrel, 1961).

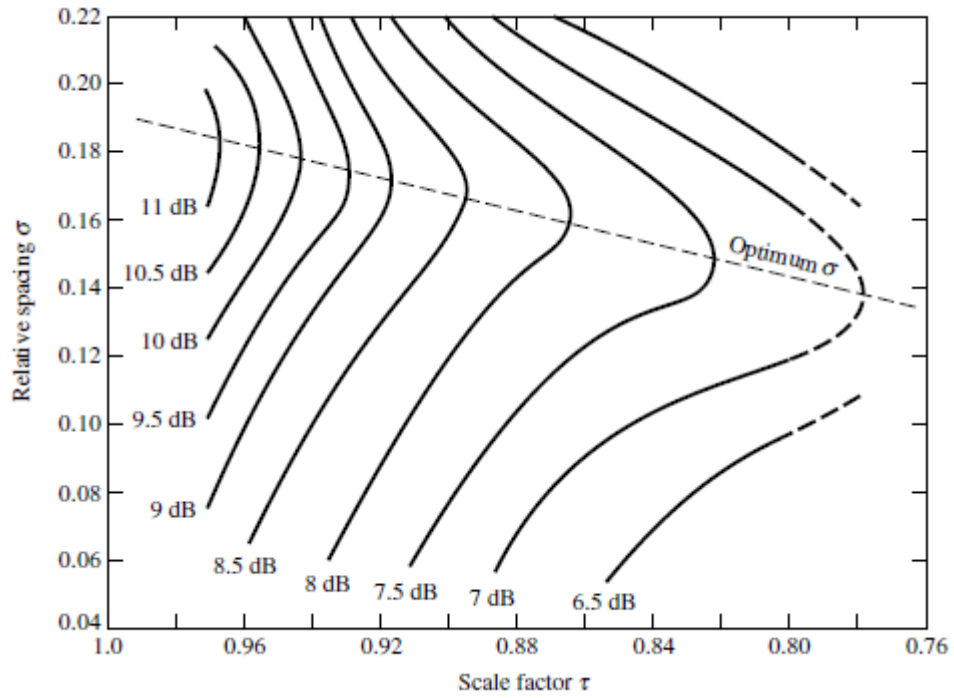


Figure 3.18 Computed contour of constant directivity versus σ and τ for log periodic dipole arrays (Balanis, 2005)

If τ become 0.88, then the ideal behavior of the log-periodic antenna is obtained (Ávila-Navarro, Blanes, Carrasco, Reig, & Navarro, 2006). Therefore, for PLPDA τ is chosen 0.88 for proper design.

Moreover, in order to design log periodic dipole array there is a number of equations should be calculated which was proposed by Carrel, (1961). Such as bandwidth of the active region B_{ar} , length of the structure (L) and average characteristic impedance of the elements Z_{ar} .

Although the lengths of the shortest and longest component of the structure are defined by the bandwidth of the system, the width of the active region depends on particular design. Equation 3.15 gives a semiempirical formula to calculate the B_{ar} .

$$B_{ar} = 1.1 + 7.7(1 - \tau)^2 \cot \alpha. \quad (3.15)$$

In practice, designed bandwidth (B_s) is usually selected as slightly larger than required (B). Equation 3.16 expresses the relationship between these quantities.

$$B_s = BB_{ar} = B[1.1 + 7.7(1 - \tau)^2 \cot \alpha]. \quad (3.16)$$

where; B_s = designed bandwidth, B = desired bandwidth, B_{ar} = active region bandwidth.

The overall length of the structure L , from the shortest (l_{\min}) to the longest (l_{\max}) element, is given by;

$$L = \frac{\lambda_{\max}}{4} \left(1 - \frac{1}{B_s}\right) \cot \alpha \quad (3.17)$$

where;

$$\lambda_{\max} = 2l_{\max} = \frac{v}{f_{\min}} \quad (3.18)$$

From the geometry of the system, the number of elements is determined by;

$$N = \frac{\ln(B_s)}{\ln(1/\tau)} \quad (3.19)$$

The necessary input impedance (assumed to be real), and the diameter of the dipole elements and the feeder-line conductors can be specified to determine the center-to-center spacing s of the feeder-line conductors. To achieve this, firstly the mean of the characteristic impedance of the elements is determined by;

$$Z_a = 120 \left[\ln \left(\frac{l_n}{d_n} \right) - 2.25 \right] \quad (3.20)$$

where ln/dn gives the length-to-diameter ratio of the n th element of the array. All elements of the array should have same the length-to-diameter ratio to design log-periodic ideally. In practice, however, the elements are generally separated into one, two, three, or many groups with all the elements in any group having the same diameter but different length. The whole number of elements of the array specifies the number of groups. In general, three groups (for the small, middle, and large elements) should be enough. In Figure 3.19, the effective loading of the dipole elements on the input line is demonstrated by the graphs.

where $\sigma' = \sigma/\sqrt{\tau}$ which is relative mean spacing, Z_a is average characteristic impedance of the elements, R_{in} is input impedance (real) and, Z_0 is characteristic impedance of the feeder line.

Balanis (2005) and Carrel (1961) give the center-to-center spacing s between the two rods of the feeder line, each of identical diameter d :

$$s = d \cosh\left(\frac{Z_0}{120}\right) \quad (3.20)$$

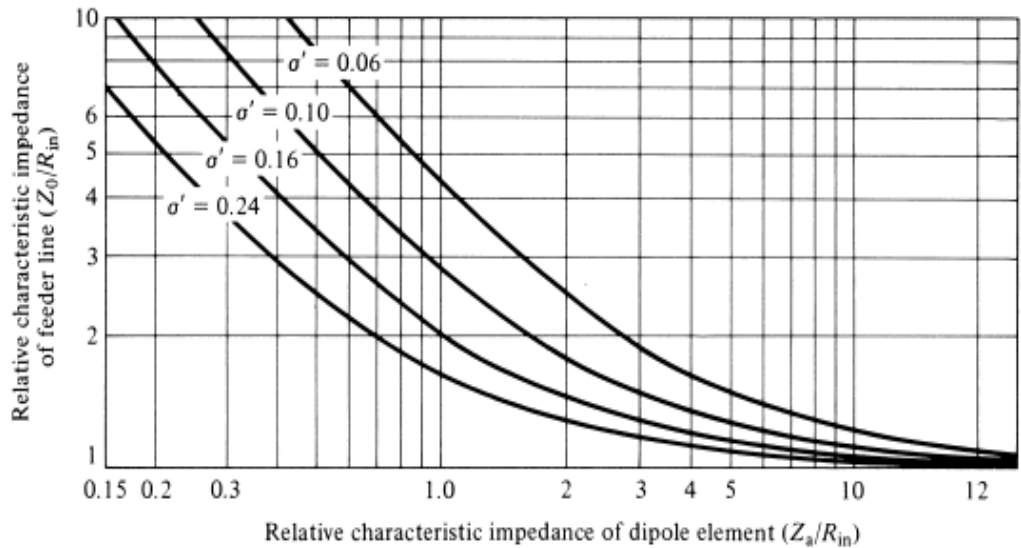


Figure 3.19 Relative characteristic impedance of a feeder line as a function of relative characteristic impedance of dipole element (Balanis, 2005)

Operating frequency of crisscross fed PLPDA is from 0.75 GHz to 3 GHz. This antenna is a part of printed antennas. Therefore, width of the characteristic impedance (W) of feed line should be calculated by (Pozar, 2012);

$$Z_o = \begin{cases} \frac{60}{\sqrt{\epsilon_{eff}}} \ln\left(\frac{8d}{W} + \frac{W}{4d}\right) & \text{For } \frac{W}{d} < 1 \\ \frac{120\pi}{\sqrt{\epsilon_{eff}} \left[\frac{W}{d} + 1.398 + 0.667 \ln\left(\frac{W}{d} + 1.444\right) \right]} & \text{For } \frac{W}{d} > 1 \end{cases} \quad (3.21)$$

where ϵ_{eff} is called effective dielectric constant.

According to Bozdağ (2014), ϵ_{eff} can be simply accepted as $\epsilon_r/2$. Table 3.5 shows value of ϵ_{eff} for FR4 and other design parameters for PLPDA. Table 3.6 gives PLPDA dimensions.

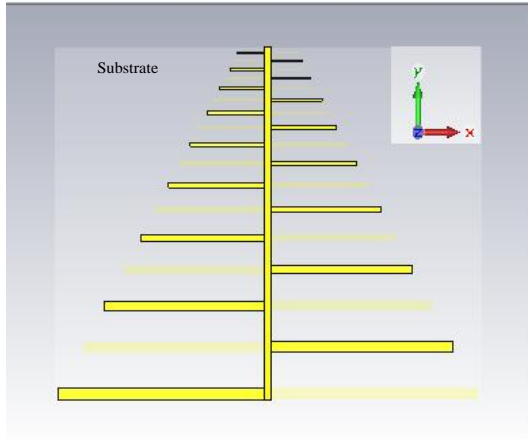
Table 3.5 Design parameters for PLPDA

ϵ_{eff}	τ	σ	α	B_{ar}	B_s	N	L	Z_a	Z_o	R_{in}	l_{max}	W
2.2	0.88	0.055	31°	1.28	5.12	17	145 mm	158.6 Ω	50 Ω	50 Ω	172 mm	3 mm

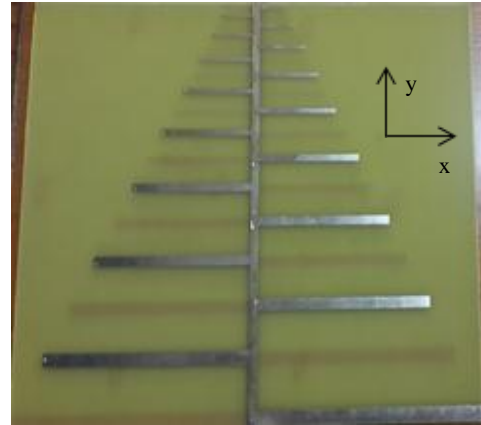
Table 3.6 PLPDA dimensions in mm (1 is the longest dipole 17 is the shortest dipole)

$L_1 = 172$	$L_{10} = 54$	$W_1 = 4.9$	$W_{10} = 1.55$
$L_2 = 152$	$L_{11} = 48$	$W_2 = 4.3$	$W_{11} = 1.36$
$L_3 = 133$	$L_{12} = 42$	$W_3 = 3.8$	$W_{12} = 1.2$
$L_4 = 117$	$L_{13} = 37$	$W_4 = 3.3$	$W_{13} = 1.05$
$L_5 = 103$	$L_{14} = 33$	$W_5 = 2.9$	$W_{14} = 0.92$
$L_6 = 91$	$L_{15} = 29$	$W_6 = 2.6$	$W_{15} = 0.81$
$L_7 = 80$	$L_{16} = 26$	$W_7 = 2.3$	$W_{16} = 0.72$
$L_8 = 70$	$L_{17} = 23$	$W_8 = 2$	$W_{17} = 0.63$
$L_9 = 62$		$W_9 = 1.77$	

Simulated and manufactured views of the printed log periodic dipole array antenna are shown in Figure 3.20.



(a)



(b)

Figure 3.20 Printed log periodic dipole array antenna (a) modeled in CST Microwave Studio, (b) realization of the antenna

Simulation and measurement results of the antenna are given following figures. Figure 3.21 gives the S_{11} performance, Figure 3.22 and Figure 3.23 gives normalized E-plane and H-plane radiation patterns respectively. Also, in Table 3.7 calculated and simulated broadside gains are given.

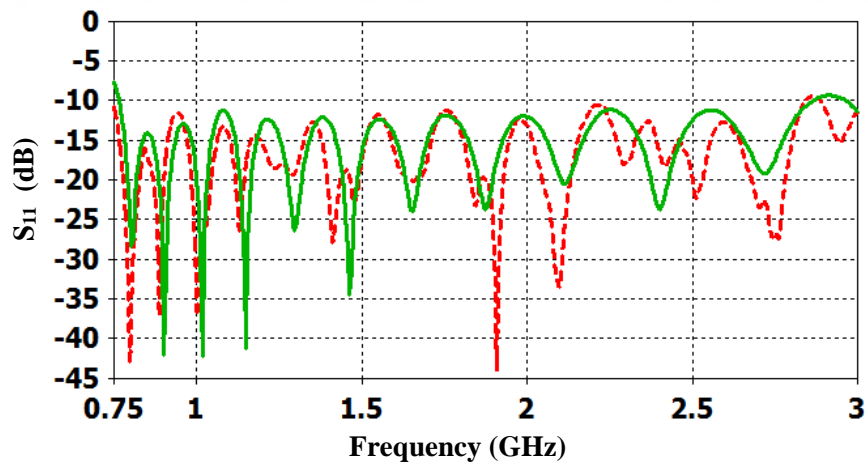


Figure 3.21 Simulation and measurement results for PLPDA (--- measurement, — simulation)

Table 3.7 Calculated and simulated broadside gains for different frequencies for PLPDA

Frequency	Calculated Gain	Simulated Gain
1 GHz	6 dB	6.5 dB
1.5 GHz	5 dB	6 dB
2 GHz	5.5 dB	5.8 dB
2.5 GHz	5.5 dB	5.1 dB
3 GHz	5 dB	4.9 dB

Measured and simulated S_{11} for PLDPA are matched well in the desired frequency range. Moreover, there are good agreements between calculated and simulated broadside gains. However, maximum 1 dB deviations are observed in the given frequencies in the Table 3.7.

According to simulated and calculated results, printed log periodic dipole array antenna has almost constant and acceptable broadside gain (~ 5.5 dB) in the given frequencies in Table 3.7.

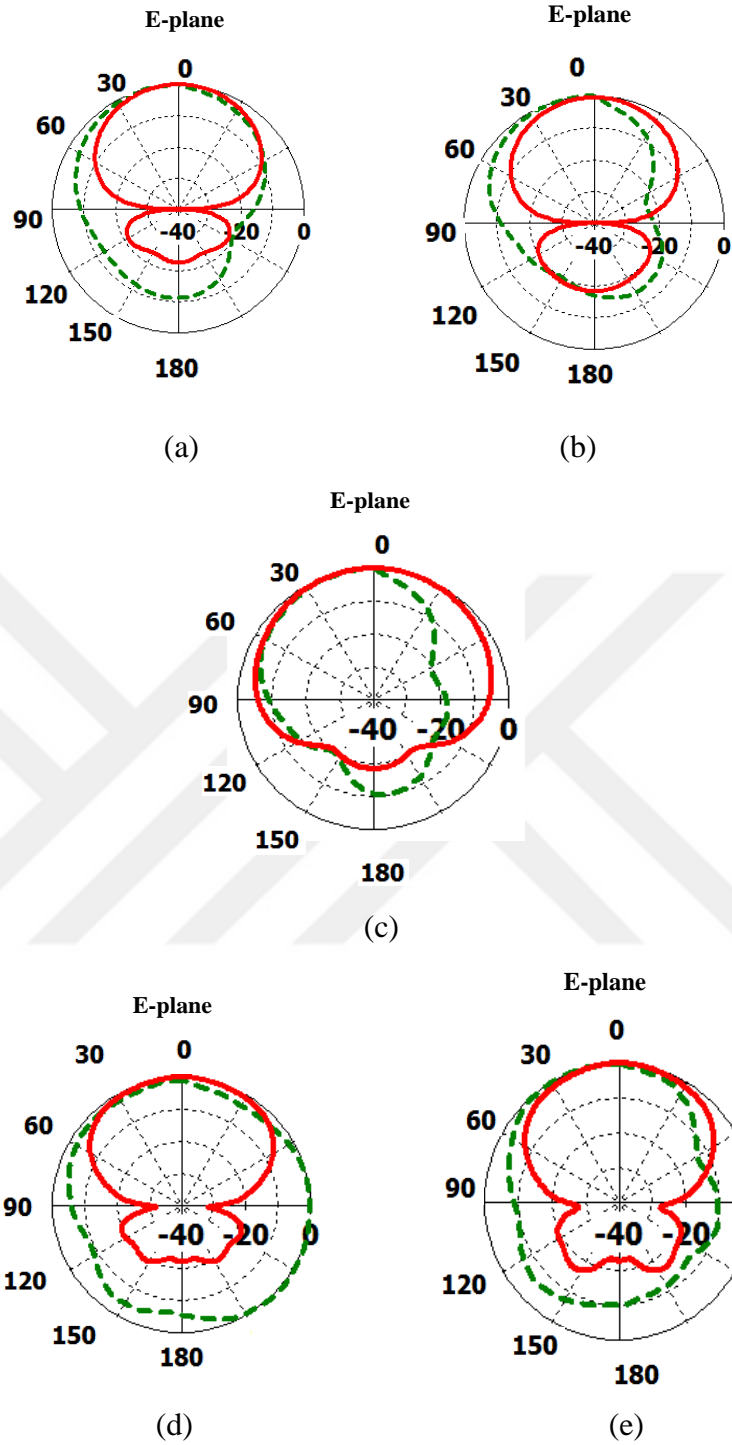


Figure 3.22 Measured and simulated E-plane of PLPDA (--- measurement, — simulation) at (a) 1 GHz, (b) 1.5 GHz, (c) 2 GHz, (d) 2.5 GHz, (e) 3 GHz

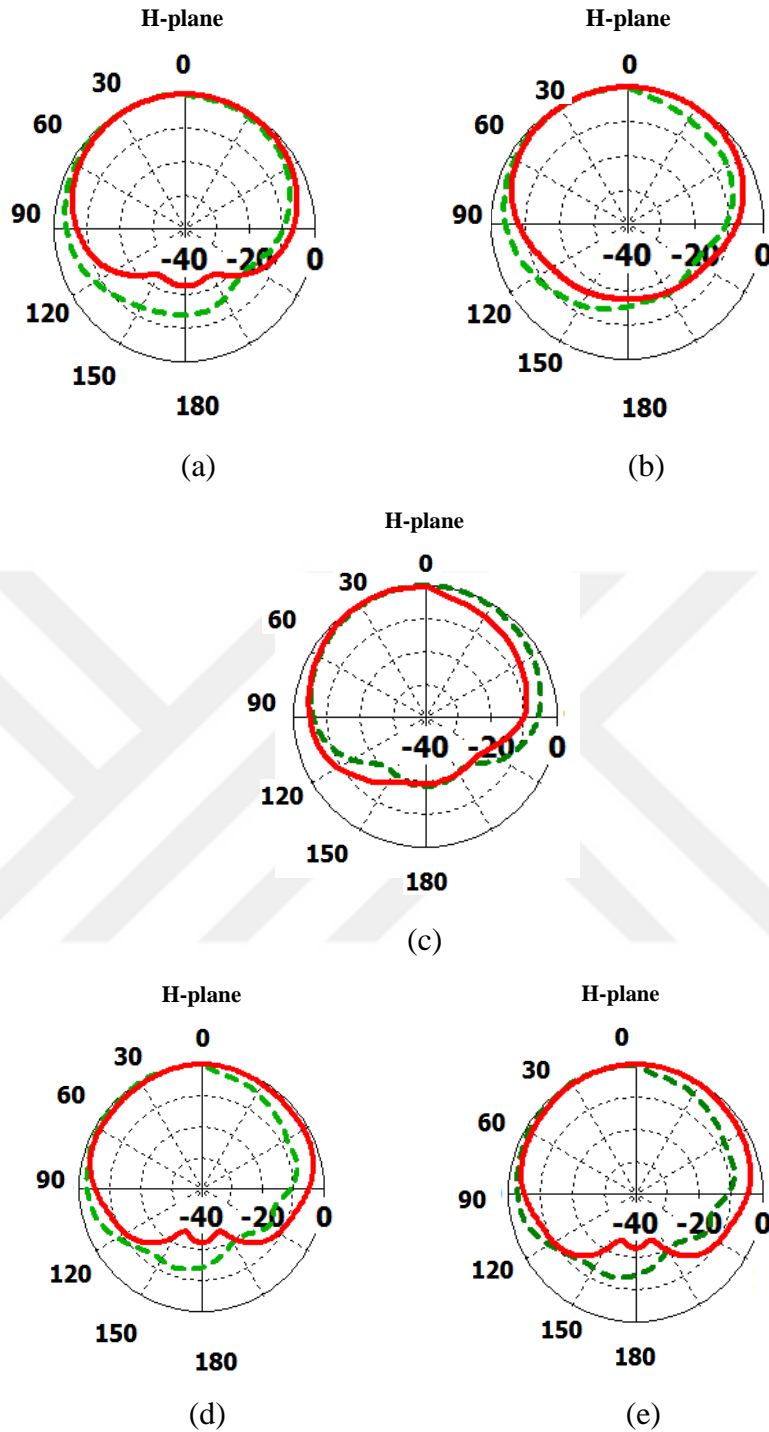


Figure 3.23 Measured and simulated H-plane of PLPDA (--- measurement, — simulation) at (a) 1 GHz, (b) 1.5 GHz, (c) 2 GHz, (d) 2.5 GHz, (e) 3 GHz

Measured normalized H-plane radiation patterns for all frequencies and normalized E-plane radiation patterns for low frequencies are matched well with simulated data. However, deviations are observed between measured and simulated

normalized E-plane radiation patterns for higher frequencies especially in 2.5 GHz. They can be caused from measurement errors or defects in cable connections.

3.5 Koch Fractal Log Periodic Dipole Array Antenna

Fractal antenna is based on concept of Fractal which is the iteration of some analogous geometric structure, it can be applied by scaling this structure and fractal was firstly described by Benoit Mandelbrot in 1975. Fractals can be divided into two categories. These are deterministic and random. Some examples of deterministic are the von Koch snowflake and the Sierpinski gaskets (Balanis, 2005; Chairunnisa, Sihaloho & Munir 2015). There are various Koch Fractal Log Periodic Antennas (KFLPA) in the literature such as Chairunnisa, Sihaloho & Munir (2015). In the thesis, a KFLPA with the dimensions of 154 mm × 151 mm × 1.6mm is designed, simulated and manufactured based on the literature. The geometry and realization of the KFLPA and simulation results are shown in Figure 3.24 and 3.25 respectively.

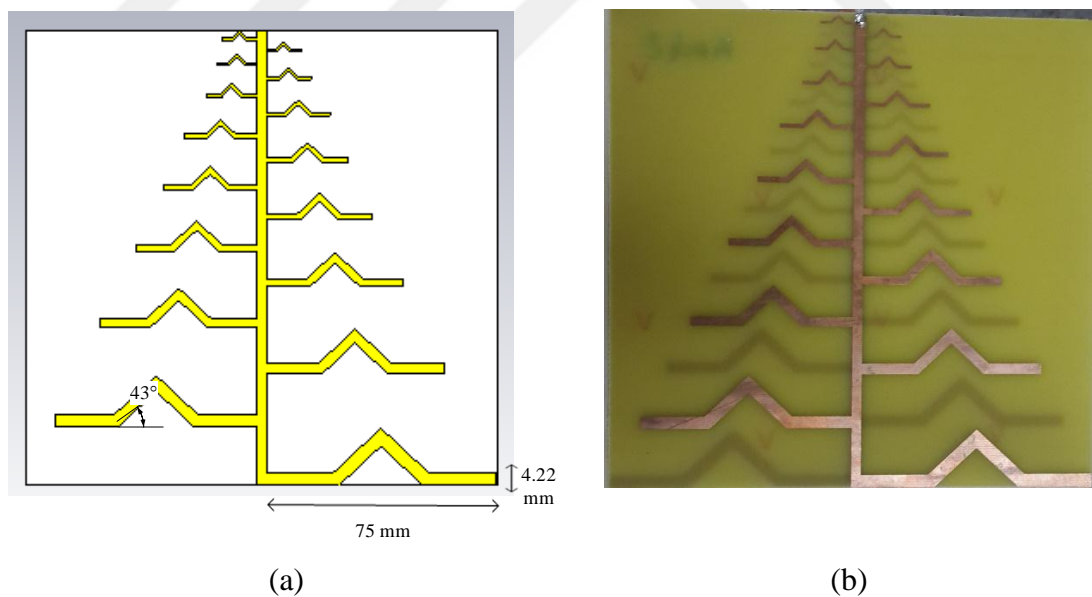
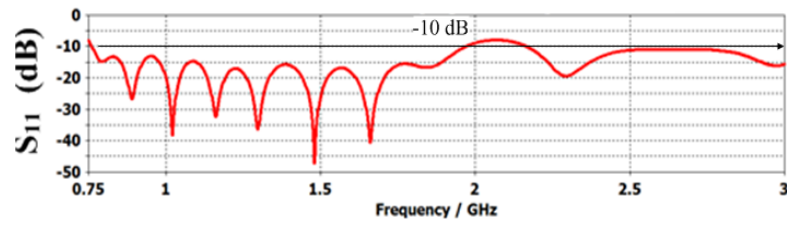
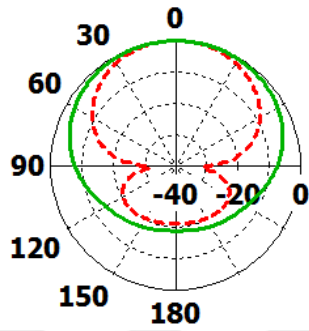


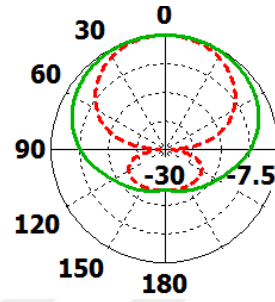
Figure 3.24 KFLPA (a) geometry, (b) realization



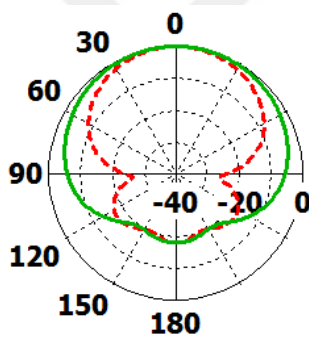
(a)



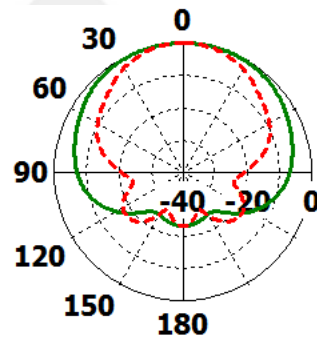
(b)



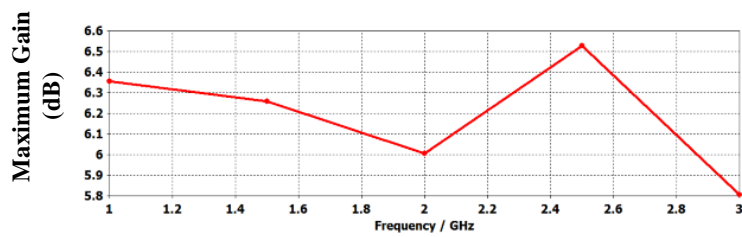
(c)



(d)



(e)



(f)

Figure 3.25 Simulation results of KFLPA (a) simulated return loss, simulated E-Plane and H-plane polar radiation patterns at (b) 1 GHz, (c) 1.5 GHz, (d) 2 GHz, (e) 2.5 GHz (--- E-Plane, — H-Plane), (f) maximum gain over frequency

CHAPTER FOUR

CONCLUSION AND FUTURE WORKS

In this thesis, the study of different types of microstrip antennas including design, simulation, realization and measurement are presented. The simulations are conducted with Finite Integration Technique based CST Microwave Studio. Antenna performance parameters such as return loss, radiation pattern and gain are taken into account for the analysis of the antennas. On the other hand, sizes of the antennas are convenient for used anechoic chamber and log periodic dipole array antennas are selected to be implemented the chamber. Some of the measurements are done in this chamber. Measurement results are compared with simulation results, and a good agreement is obtained. Each antenna almost operates from 0.75 GHz to 3 GHz, which is suitable for GSM (900 MHz), GPS (1575.42 MHz, 1227.60 MHz), 3G (2100 MHz), Wi-Fi (2400 MHz), and LTE (2600 MHz) wireless systems.

The first type of antenna studied in the thesis is the printed planar monopoles. They have many desired features such as simple structure, broad bandwidth, and ease of printing on a dielectric substrate. These features make them an important candidate for many communication systems. In this study, printed planar monopole antennas containing two different types are simulated, fabricated and measured. Although the performances of these antennas can be considered to be satisfactory for anechoic chamber measurement, they have drawbacks of being frequency dependent, radiation pattern. Main lobe shifts when frequency changes.

- The first printed planar monopole antenna is based on printed circular disc. The parameters of the antenna are optimized for the desired operating frequency range. Finally, total length and width of the antenna are determined as 157 mm and 116 mm, respectively. According to the simulation and measurement results, the antenna almost satisfies desired conditions. However, main lobe of the antenna shifts when frequency changes.

- In the second printed monopole antenna, a broadband modified rectangular microstrip-fed monopole antenna using stepped cut at four corners (SCFC) method is used, and T-shape slot is employed to the ground to increase bandwidth at the desired frequency range. Total length of the antenna is 150 mm, and total width of the antenna is 104 mm. Simulation and measurement results show that desired results are almost achieved also in this antenna. However, main lobe of the antenna shifts when frequency changes.

Other type of antenna studied in this thesis is the printed log periodic dipole array, which is selected due to having large bandwidth, with a reasonable gain, having directional radiation pattern, having low production cost and being suitable for many applications. In the study, printed log periodic dipole array antennas are simulated, manufactured and measured. According to results, these antennas are more suitable to anechoic chamber measurements as compared to monopole antennas. This is because, radiation pattern of the log periodic antennas is more frequency independent than monopole ones.

- A printed log periodic dipole array is designed by the help of standard log periodic dipole array antenna formulations with some modifications. The designed antenna has 17 printed dipoles. Dipoles are printed both side of the FR4 substrate symmetrically. The largest dipole is designed for 0.75 GHz that is minimum operating frequency and the shortest dipole is designed for 3 GHz that is the maximum operating frequency. Total length of the antenna is 147 mm and total width of the antenna is 174 mm. Simulation and measurement results demonstrate that the desired specifications are almost satisfied.

Finally, a Koch Fractal Log Periodic Array Antenna with dimensions of 154 mm × 151 mm × 1.6 mm is designed, simulated and manufactured. The designed antenna has 17 printed dipoles. According to simulation results this antenna has directional radiation pattern, almost constant and desirable broadside gain in the operating frequency band.

Printed log periodic dipole array antennas are implemented to the anechoic chamber due to having directional radiation pattern, almost constant and acceptable broadside gain (~ 5.5 dB) in all operating frequency band.

As a future work, size reduction or pattern improvement methods can be employed to the antennas. Some methods have been conducted to miniaturize size of the antenna are using EBG (Electromagnetic Band Gap) or AMC (Artificial Magnetic Conductor) structures. AMC and EBG structures are periodic repetitions of unit cell which are geometrical arrangement materials such as dielectrics, conductors. Almutawa (2011), presents a study about Log-periodic microstrip patch antenna miniaturization using AMC surfaces and Abbasi & Langley (2010), propose (AMC)-based multiband low-profile antenna.

Moreover, as a part of future work, KFLPA antenna can be measured. Also, KFLPA antenna with series iteration can be designed such as Karim, Rahim, Majid, Ayop, Abu & Zubir (2010).

To sum up, wideband printed planar monopole antennas with nearly omnidirectional radiation pattern and a printed log periodic dipole array antenna with directional radiation pattern are designed, simulated, manufactured on FR4 substrate and measured. Measurement results are compared with simulation results. There is almost a good agreement. Finally, a Koch Fractal log periodic dipole array antenna is designed, simulated and fabricated.

REFERENCES

- Abbasi, N.A., & Langley, R.J. (2010). Multiband-integrated antenna/artificial magnetic conductor. *IET Microwaves, Antennas & Propagation*, 5 (6), 711-717.
- Agrawall, N. P., Kumar, G. & Ray, K. P. (1998). Wideband planar monopole antennas. *IEEE Transactions on Antennas and Propagation*, 46 (2), 294-295.
- Almutawa, A. T. (2011). *Log-periodic microstrip patch Antenna miniaturization using artificial magnetic conductor surfaces*. M.Sc Thesis, University of South Florida, Florida.
- Ammann, M. (1999). Square monopole planar antenna. *IEE National Conference on Antennas and Propagation*, 37-40.
- Anritsu (2015). *MS4640B Series*. Retrieved December 1, 2015, from <https://www.anritsu.com/en-US/test-measurement/products/MS4640B-Series#>
- Ávila-Navarro, E., Blanes, J. A., Carrasco, J. A., Reig, C. & Navarro, E. A. (2006). A new bi-faced log periodic printed antenna. *Microwave and Optical Technology Letters*, 48 (2), 402-405.
- Ávila-Navarro, E., & Reig, C. (2012). Directive microstrip antennas for specific below- 2.45 GHz applications. *International Journal of Antenna and Propagation*, 2012.
- Balanis, C. A. (2005). *Antenna theory analysis and design*. United States: John Wiley & Sons.
- Bozdağ, G. (2014). *Novel microstrip antennas for multiband and wideband applications*. M.Sc Thesis, İzmir Institute of Technology, İzmir.

- Çakır, G. (2004). *Gezgin iletişim sistemleri için hüzme yönlendirmeli mikroşerit anten tasarımı: Analitik hesaplama, bilgisayar benzetimleri ve ölçümleri*. Ph.D. Thesis, Kocaeli University, Turkey.
- Carrel, R. (1961). The design of log-periodic dipole antennas. *IRE International Convention Record*, 61-75.
- Casula, G. A., Maxia, P., Mazzarella, G. & Montisci, G. (2013). Design of a printed log-periodic dipole array for ultra-wideband applications. *Progress in Electromagnetics Research C*, 38, 15-26.
- Chairunnisa, Sihaloho, D. F., & Munir, A. (2015). Size reduction of printed log-periodic dipole array antenna using fractal koch geometry. *International Journal on Electrical Engineering and Informatics*, 7 (2), 226-236.
- Chaiteang, N., Ghankaew, P., Chareonsiri, P., & Thaiwirot, W. (2014). Design of a compact printed wide-slot antenna for WLAN applications. *Electrical Engineering/Electronics, Computer, Telecommunications and Information Technology (ECTI-CON), 2014 11th International Conference on* (1-4).
- Chan, C. W. (2011). *Investigation of propagation in foliage using simulation techniques*. M.Sc Thesis, Naval Postgraduate School: California.
- Chen, Z.N., & Chia, M.Y.W. (2006). *Broadband planar antennas design and applications*. United States: John Wiley & Sons.
- CST (2014). *Antenna design and simulation*. Retrieved September 15, 2014, from <https://www.cst.com/Applications/Category/Antenna+Design+and+Simulation>.
- CST (2014). *CST Microwave Studio*. Retrieved September 15, 2014, from <https://www.cst.com/Products/CSTMWS>.

- Curwen, P., & Whalley, J. (2013). *Fourth generation mobile communication: the path to superfast connectivity*. Switzerland: Springer.
- Davidson D. B. (2005). *Computational electromagnetics for RF and microwave engineering*. United States: Cambridge University Press.
- Dubost, G., & Zisler, S. (1976), *Antennas a large band.*, United States: New York.
- DuHamel, R. H., & Isbell, D. (1957). Broadband logarithmically periodic antenna structures. *IRE International Convention Record*, 5, 119-128.
- Emerson, W. H., & Sefton, H. B. (1965). An improved design for indoor ranges. *Proceeding*, 53, 1079–1081.
- Evans, J. A., & Ammann, M. J. (2004). The effect of element width on the impedance bandwidth and mode for the rectangular monopole antenna. In *URSI International Symposium on Electromagnetic Theory*, 580-583.
- Garg R., Bhartia, P., Bahl, I., & Ittipiboon, A. (2001). *Microstrip antenna design handbook*. United States: Artech House.
- Gillette, M. R., & Wu, P. R. (1977) RF anechoic chamber design using ray tracing. In *Antennas and Propagation Society International Symposium*, 15, 246-249.
- Hassanien, M. A., & Hamad, E. K. I. (2010). Compact rectangular u-shaped slot microstrip patch antenna for UWB applications. *Middle East Conference on Antennas and Propagation (MECAP)*, 1-4.
- Howell, J. Q. (1972). Microstrip antennas. *IEEE Antennas and Propagation Society International Symposium Digest*, 177–180.

Huang, C. F., & Huang, Y. F. (2012). Design of RFID reader antenna for exclusively reading single one in tag assembling production. *International Journal of Antennas and Propagation*, 2012.

International Telecommunication Union (ITU). (2003), *Frequency arrangements for implementation of the terrestrial component of International Mobile Telecommunications-2000 (IMT-2000) in the bands 806-960 MHz, 1710-2025 MHz, 2110-2200 MHz and 2500-2690 MHz*. Retrieved August 12, 2015, from https://www.itu.int/dms_pubrec/itu-r/rec/m/R-REC-M.1036-2-200306-S!!PDF-E.pdf.

James, J. R., & Hall, P. S. (1989). *Handbook of microstrip antennas*. United Kingdom: IEE Electromagnetic Waves Series.

Jiao, J. J., Zhao, G., Zhang, F. S., Yuan, H. W., & Jiao, Y. C. (2007). A broadband CPW-fed T-shape slot antenna. *Progress In Electromagnetic Research*, 76, 237-242.

Kahnert, F. M. (2002). Numerical methods in electromagnetic scattering theory. *Journal of Quantitative Spectroscopy and Radiative Transfer*, 79, 775-824.

Karim, M. N. A., Rahim, M. K. A., Majid, H. A., Ayop, O., Abu, M., & Zubir, F. (2010). Log periodic fractal koch antenna for UHF band applications. *Progress In Electromagnetics Research*, 100, 201-218.

Koyya, L., Lakshmi, R., & Raju, G. (2013) Optimization of geometry of microstrip patch antenna for broadband applications. *International Journal of Advanced Research in Electrical, Electronics and Instrumentation Engineering*, 2 (7), 3119-3122.

Lee, C. C., Huang, H. S., Yang, C. D., & Wang, C. W. (2008). An experimental study of the printed-circuit elliptic dipole antenna with 1.5-16 GHz bandwidth.

- International Journal of Communications, Network and System Sciences*, 1 (04), 295.
- Liang, J. (2006). *Antenna study and design for ultra wideband communication applications*. Ph.D Thesis, Queen Mary University of London, London.
- Liang, J., Chiau, C. C., Chen J., & Parini, C. G. (2005). Study of a printed circular disc monopole antenna for UWB systems. *Antennas and Propagation*, 53 (11), 3500-3504. IEEE.
- Meinke, H., & Gundlach, F. W. (1968). Taschenbuch der hochfrequenztechnik. *Springer-Verlag*, 531-535, Microstrip Patch Antenna. *IEEE Transactions* 49 (6), 849-854.
- Mondal, K., & Sarkar, P. P. (2014). Design of compact broadband high gain microstrip patch antennas with modified ground plane. *Microwave and Optical Technology Letters*, 56 (5), 1255-1259.
- Moradikordalivand, A., Rahman, T. A., Ebrahimi S., & Hakimi, S. (2014). An equivalent circuit model for broadband modified rectangular microstrip-fed monopole antenna. *Wireless Personal Communications*, 77 (2), 1363–1375.
- Morgan, D. (2007). *A handbook for EMC testing and measurement* (Paperback Ed.) London: The Institution of Engineering and Technology (The IET).
- Munson, R. E. (1974). Conformal microstrip antennas and microstrip phased arrays. *IEEE Transactions on Antennas and Propagation*, AP, 74–78.
- Nakar, P. S. (2004). *Design of a compact microstrip patch antenna for use in wireless/cellular devices*. M.Sc Thesis, Florida State University, Florida.

Poole, I. (n.d). *RF network analyzer basics tutorial*. Retrieved September 12, 2015, from http://www.radio-electronics.com/info/t_and_m/rf-network-analyzer/analyser-basics-tutorial.php.

Poole, I. (n.d.). *Vector network analyzer VNA tutorial*. Retrieved September 14, 2015, from http://www.radio-electronics.com/info/t_and_m/rf-network-analyzer/vector-analyser-vna-tutorial.php.

Powell, J. (2004). *Antenna design for ultra wideband radio*. M.Sc Thesis, Massachusetts Institute of Technology, Massachusetts.

Pozar, D. M. (1983). Considerations for millimeter wave printed antennas. *Antennas and Propagation, IEEE Transactions on*, 31 (5), 740-747.

Pozar, D. M. (2001). *Microwave and RF design of wireless systems* (1th Ed.). United States : John Wiley & Sons.

Pozar, D. M. (2012). *Microwave engineering* (4th Ed.). United States: John Wiley & Sons.

Rahimi, J. (2011). *The finite integration technique (FIT) and the application in lithography simulations*. Ph.D Thesis, University of Erlangen-Nuremberg, Nürnberg.

Seçkin Uğurlu, Ş., Özgönül, M. C., Özkurt, A., & Seçmen, M. (2015) An RF anechoic box system development for shielding effectiveness measurements. *The 9th International Conference on Electrical and Electronics Engineering ,ELECO*, 209.

Seçmen, M. (2011). *Multiband and wideband antennas for mobile communication systems, recent developments in mobile communications. A multidisciplinary approach*, Dr Juan P. Maicas (Ed.). Croatia: InTech.

- Stutzman, W. L., & Thiele, G.A. (2013). *Antenna theory and design* (3rd Ed.). United States: John Wiley & Sons.
- Taflove, A. (1998). *Advances in computational electrodynamics: the finite difference time domain method.*, Boston: Artech House.
- Tamaoka, H.A., Hamada, H., & Ueno, T. (2004). Multiband antenna for mobile phones. *Furukawa Review*, (26), 12-16.
- Taove, A., & Hagness, S. C. (2000). *Computational electrodynamics: the finite-difference time-domain method.* Boston, London: Artech House.
- The International Engineering Consortium (n.d.). *Global system for mobile communication (GSM)*. Retrieved June 5, 2015, from <http://www.uky.edu/~jclark/mas355/GSM.PDF>.
- Ulaby, F.T. (2007). *Fundamentals of applied electromagnetics* (5th Ed.). United States: Pearson Education Inc.
- University of California, Irvine Environmental Health & Safety; Radiation Safety Division, (2008). *What is Wi-Fi and is it safe ?* Retrieved May 7, 2015, from <https://www.ehs.uci.edu/programs/radiation/Wi-Fi%20Safety.pdf>.
- Volakis, J.L. (2007). *Antenna engineering handbook*. United States: McGraw Will.
- Waterhouse, R., & Novak, D. (2007). *Printed antennas for wireless communications edited by Rod Waterhouse*. England: John Wiley & Sons.
- Yadav, A., & Pahwa, K. (2014). Design & parametric study of rectangular slot microstrip patch antenna for uwb applications. *International Journal of Electrical & Electronics Engineering*, 1 (3), 1694-2426.

Yıldırım, M. (2010). *Design of dual polarized wideband microstrip antennas*. M.Sc Thesis, Middle East Technical University, Ankara.

Zyren, J. (2007). *Overview of the 3GPP long term evolution physical layer*. United States: Freescale Semiconductor, Incorporated.

